OPEN ACCESS
IOP Publishing | London Mathematical Society Nonlinearity
Nonlinearity **34** (2021) 8248–8282 https://doi.org/10.1088/1361-6544/ac2e44

# Capturing the cascade: a transseries approach to delayed bifurcations

**Inês Aniceto[1,*], Daniel Hasenbichler[1], Christopher J Howls[1] and Christopher J Lustri[2]**

[1] Mathematical Sciences, University of Southampton, Highfield, Southampton, SO17 1BJ, United Kingdom
[2] Department of Mathematics and Statistics, 12 Wally's Walk, Macquarie University, New South Wales 2109, Australia

E-mail: i.aniceto@soton.ac.uk

Received 12 February 2021, revised 6 September 2021
Accepted for publication 8 October 2021
Published 2 November 2021

**Abstract**

Transseries expansions build upon ordinary power series methods by including additional basis elements such as exponentials and logarithms. Alternative summation methods can then be used to 'resum' series to obtain more efficient approximations, and have been successfully widely applied in the study of continuous linear and nonlinear, single and multidimensional problems. In particular, a method known as transasymptotic resummation can be used to describe continuous behaviour occurring on multiple scales without the need for asymptotic matching. Here we apply transasymptotic resummation to discrete systems and show that it may be used to naturally and efficiently describe discrete delayed bifurcations, or 'canards', in singularly-perturbed variants of the logistic map which contain delayed period-doubling bifurcations. We use transasymptotic resummation to approximate the solutions, and describe the behaviour of the solution across the bifurcations. This approach has two significant advantages: it may be applied in systematic fashion even across multiple bifurcations, and the exponential multipliers encode information about the bifurcations that are used to explain effects seen in the solution behaviour.

Keywords: logistic equation, transseries, delayed bifurcations, series summation, difference equation

Mathematics Subject Classification numbers: 39A28, 41A69, 40A25, 40G99.

*Author to whom any correspondence should be addressed.
Recommended by Dr Reiner Lauterbach.

(Some figures may appear in colour only in the online journal)

## 1. Introduction

Transseries are a natural extension to classical asymptotic power series which are used to study systems in which the solution behaviour depends on multiple distinct exponential scales. A transseries represents the solution to a system as the sum of multiple power series, each multiplied by a different exponential prefactor [29]. The value in this approach is that a transseries developed in one region of parameter space can typically be extended into regimes in which the solution depends on different scales, simply be applying different summation methods to the transseries itself, without the need to rebalance the equation terms and apply matched asymptotic expansions to connect the regimes.

Transseries and summation techniques have been used to study the behaviour of a wide range of parameter-dependent continuous systems. Applications include the study of general nonlinear ordinary differential equations [13, 14, 44, 55], the first Painlevé equation [5, 36, 56], topological string theory [19, 40], field theory and semi-classical quantum mechanics [4, 9, 24, 27, 39, 51], relativistic hydrodynamics and Einstein partial differential equations [3, 12, 43], and $q$-series and knot invariants [26, 35]. More recently transseries methods have been extended to study of discrete problems, such as particular matrix models governed by the first discrete Painlevé equation [5, 20, 52, 57, 58]. The role of exponential scales in discrete maps and chaos has been previously analysed in the context of Stokes phenomena [37, 41, 53, 59].

The transasymptotic method introduced in [14–16] consists of constructing a transseries in terms of some small parameter $\varepsilon$. The transseries terms are then reordered, and higher-order exponential terms at each order of the small parameter are summed. This change of summation order, or 'resummation', captures the behaviour of the system in regions where different exponential terms dominate the solution. Transasymptotic methods have been used to determine the location of moveable poles in Painlevé equations directly from asymptotic solutions [6, 16] (see also [17, 18]). In this work, we show that these transseries and summation approaches can be used in a systematic fashion to identify complicated bifurcations in discrete systems that typically require careful application of multiple scales [42] or renormalisation methods [8].

In this study, we demonstrate that transseries resummation can be used systematically to accurately capture the behaviour of the solution to a discrete equation containing a periodic-doubling cascade with delayed bifurcations. Such a solution is illustrated in figure 1, which shows a solution to the slowly varying logistic equation, given in (1) with $\lambda = 3 + \varepsilon n$. The aperiodic[3] solution manifold is unstable for $\lambda > 3$, corresponding to $n = 0$. The solution behaviour does not immediately become two-periodic at $n = 0$. Instead, the behaviour remains close to the unstable aperiodic manifold before jumping rapidly to the two-periodic stable manifold at $n \approx 300$. Similar behaviour may be seen in the jump from two-periodic to four-periodic behaviour in the solution. The two-periodic manifold becomes unstable at $n = 3122$; however, solution begins to demonstrate visible four-periodic behaviour in a rapid change at $n \approx 3500$. These jumps are examples of delayed period-doubling bifurcations.

[3] It would be consistent with other terminology of this paper to refer the single-valued solution manifold as 'one-periodic', to be consistent with the use of '$n$-periodic' to describe the multi-valued solution manifolds. We instead choose 'aperiodic' to emphasise that solutions on this manifold do not contain discrete-scale variation.

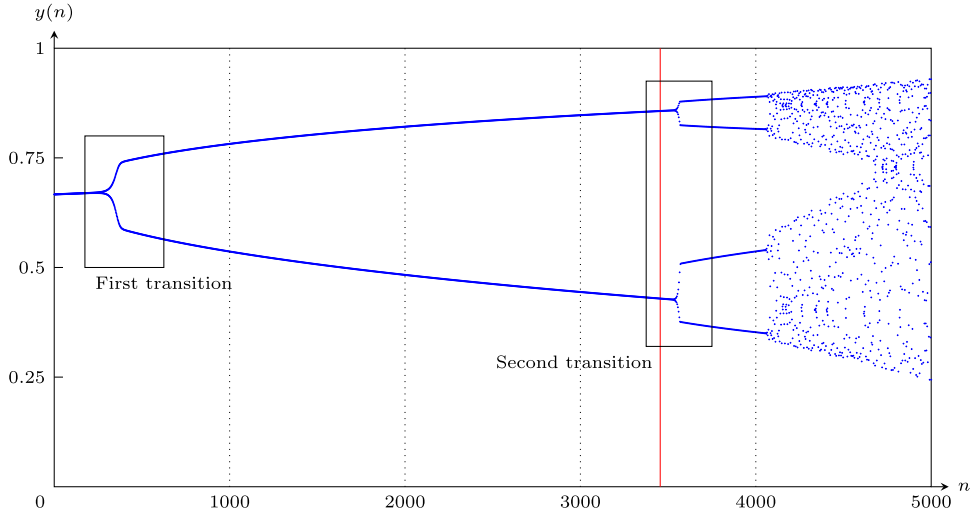


**Figure 1.** Solution to logistic equation (1), where $\lambda = 3 + \varepsilon n$ with $\varepsilon = 0.001\,44$. The period-doubling cascade is apparent; the transition between aperiodic and two-periodic behaviour is visible, as is the transition between two-periodic and four-periodic behaviour. As the solution continues, it eventually becomes chaotic. The two-periodic behaviour in the solution begins to contribute immediately, but is not immediately visibly apparent due to the delay in the bifurcation behaviour. From exponential weights associated with the four-periodic solution, calculated in (89) and depicted in figure 7, we will determine that solution begins to display four-periodic behaviour at $n \approx 3455$, but that it will not immediately be visible. This value of $n$ is marked with a red line, and the jump becomes apparent soon after this point.

Delayed bifurcations may occur in dynamical systems where an underlying parameter is itself slowly varying and the solution initially clings to a metastable branch of the solution before eventually jumping to the stable branch. They have been studied widely in systems of ordinary differential equations (see, for example [63]). These 'slow-fast' systems have behaviour occurring on two (or more) distinct timescales, with the solution trajectory remaining near to an unstable solution for a significant distance after stability has been lost; solutions containing this behaviour have been termed 'canards'.

There has been a significant volume of work studying the asymptotic behaviour of canards in continuous settings, see for example, using composite asymptotic expansions in [10, 28, 33], steepest descent analysis [38], and Borel summation methods in [25]. Borel summation methods are closely connected to transseries resummation methods (see [2]), and have been used to study discrete problems, as in [54]. This motivates the idea that transseries resummation methods could be a useful technique for studying delayed bifurcation behaviour. In the present study, we will focus on delayed bifurcations appearing in discrete systems, and in particular, singularly perturbed variants of the logistic map.

We will show that period doubling bifurcations depend on the interaction between different exponential factors, and it is therefore advantageous to represent them explicitly using transseries. By expanding in the asymptotic limit, we may determine terms in the algebraic power series to determine the initially stable aperiodic solution. The next step will be to reorder the transseries terms and perform a transasymptotic resummation, which will produce an accurate description of the doubling phenomena. This approach has the additional advantage that

it allows us to determine further subdominant exponential scales in the transseries explicitly which dictate subsequent doubling bifurcations present in the solution.

By incorporating a multiple scales ansatz into the transseries expression, we will shown that transseries resummation—which was developed to describe continuous behaviour—can be used to calculate discrete variation without any further analysis to the transseries method.

We study here two variants of the ubiquitous (and generic) standard logistic map

$$y(n+1) = \lambda y(n)\,[1 - y(n)]\,, \quad 0 < y(0) < 1, \tag{1}$$

where $\lambda$ is a dimensionless bifurcation parameter $0 < \lambda \leqslant 4$. If $y(0)$ is selected from outside this range, the map becomes unbounded as $n$ increases.

This system contains a period-doubling route to chaos, found by allowing the parameter $\lambda$ to vary. In the range $1 < \lambda < 3$, this system tends to a stable equilibrium without periodic effects. In the range $3 < \lambda < 1 + \sqrt{6}$, the system tends to a two-periodic stable equilibrium. Increasing $\lambda$ beyond $1 + \sqrt{6}$ produces systems that tend to stable equilibria with higher periodicity. For $\lambda > 4$, the map is unbounded for large $n$, and does not demonstrate chaotic behaviour. Period-doubling may be seen for negative values of $\lambda$ in the range $-2 < \lambda < -1$, but we will not consider these values here.

The earliest study of the delayed bifurcations in the slowly-varying logistic map is [8], who applied renormalisation methods to derive asymptotic scaling laws for the delays between period doubling, and performed analysis and numerical experiments to determine the location of the bifurcation points. In addition to establishing specific results about the slowly-varying logistic map, this study established that delayed bifurcations can play an essential role in the behaviour of discrete systems. Similar methods were used to study delayed bifurcations in more general unimodal maps [21], as well as discrete maps with noise [7, 22, 23].

Further studies of this system appeared in subsequent years. In [30, 31, 33], the existence of canard solutions was rigorously proven in general classes of discrete maps that include the slowly-varying logistic map. Further discussions of canard solutions to both discrete continuous and discrete dynamical systems are given in [32, 34].

In more recent years, this system was studied using matched asymptotic expansions and multiple scales methods [42]. The purpose of this previous work was to show that the method of multiple scales could be used to combine a 'fast' discrete timescale with a slow time variable that could be treated as continuous, while still capturing the essentially discrete-scale behaviour present in the problem. By carefully balancing terms, the authors were able to identify the bifurcation points and produce accurate asymptotic approximations to the solution behaviour on both sides of the delayed bifurcation. In the works described here, the slowly-varying logistic equation has provided a useful testing ground for treatments of discrete systems, due to the complicated behaviour that it produces.

In addition to the slowly-varying logistic equation, multiple scales-based approaches which describe a system in terms of a fast discrete timescale and a slow continuous timescale have been used to study asymptotic effects in a number of other discrete systems. This includes the study of Stokes phenomena in discrete Painlevé equations [46, 48, 49], Frenkel–Kontorova models [50], and discrete variants of the Korteweg–de Vries equation [47] and nonlinear Schrödinger equation [1].

It has been shown in [44] that transseries approaches may be used to improve upon asymptotic results obtained using matched asymptotic expansions. In that study, transseries resummation methods were used to obtain a uniform approximation to a continuous problem that had been previously solved using multiple scales methods. The transseries approach was able to naturally incorporate higher exponential terms, and thereby improve on the accuracy of the results, even for values of the perturbation parameter that were not extremely small. Motivated

by this result, we will show that transseries resummation can be used to improve on existing multiple scales results in discrete systems.

In section 2 we will first study the 'static' logistic map, corresponding to $\lambda = 3 + \varepsilon$ for a fixed choice of (small) real parameter $\varepsilon$. This will be used to introduce and to demonstrate the technical details of the transseries process.

The second variant, studied in section 3, is the 'dynamical' logistic equation, which has a slowly increasing bifurcation parameter $\lambda = 3 + \varepsilon n$. In this case, the bifurcation parameter grows, with different solutions becoming stable and unstable as $n$ increases. This behaviour, described earlier, is illustrated in figure 1 for $\varepsilon = 0.001\,44$. The first change in stability occurs for $\lambda = 3$, corresponding to $n = 0$. The second change in stability occurs for $\lambda = 1 + \sqrt{6}$, corresponding to $n = 3122$. In each case, the jump to two- and four-periodic behaviour does not occur at this value of $n$, but is delayed, appearing as a rapid jump at $n \approx 300$ and $n \approx 3500$ respectively.

Apart from the pedagogical aspects of demonstrating the applicability of transseries to such problems to recover and extend existing results, in this work we demonstrate four main enhancements.

Firstly, we show that transseries resummation can capture the behaviour of solutions to both a static and slowly-varying logistic map in a systematic and efficient fashion. The multiple scales method used by [42] was able to produce asymptotically valid approximations to the solution, but the process requires a careful expansion and asymptotic matching each time a bifurcation occurs. The transseries resummation approach used here is systematic, without any need for matching, and can be applied in largely identical fashion to capture each successive bifurcation.

Secondly, transseries resummation allows us to capture behaviour when the bifurcation parameter is not necessarily small. In [42], the static logistic map was studied in the limit that the bifurcation parameter was close to three, leading to two-periodic behaviour in the static map. In this study, the transseries resummation approach allows for the study of larger values of the bifurcation parameter, describing four- and eight-periodic behaviour in the static map.

Thirdly, we demonstrate that transseries can capture and control the onset of period-doubling behaviour through in terms of exponential weights in the transseries coupled with their resummation. By studying these exponential terms, we are able to determine precisely when higher-periodicity behaviour appears in the solution, and when the bifurcation starts to grow. We will show that transseries resummation can approximate the behaviour of two- and four-periodic solutions, and that calculating the transseries exponential terms can explain the onset of higher four- or even eight-periodic behaviour as the bifurcation parameter grows. In principle the method could be continued in the same fashion to determine this behaviour as the dynamic map sweeps through subsequent bifurcations.

Fourthly, we are able to use transseries summation to significantly improve the approximation accuracy of the solutions over and above that afforded by matched asymptotics in several parameter regimes, with minimal, if any, additional effort. The increase in accuracy is a consequence of the inclusion of multiple exponential scales in the solution approximation, and is most apparent in parameter regimes in which different exponential scales all contribute to the solution behaviour.

### *1.1. Outline of the transseries and transasymptotic methodology*

We first summarise the general methodology that we will study the logistic map (1) using transseries and summation techniques, and explain how this is able to identify origin of delayed period-doubling bifurcations in the solution. We will consider two variants of this map. This

first, in which $\lambda$ depends on a small $\varepsilon$, is denoted here as the static case, or both $n$ and $\varepsilon$, denoted here as the dynamic case.

*1.1.1. Transasymptotic method for studying the onset of two-periodic behaviour.* The logistic map is a discrete problem, while transseries and summation techniques were developed to study problems in continuous settings. We will therefore introduce a continuous parameter $x = n\varepsilon$, where $\varepsilon$ is taken to be a small parameter, and analyse the problem

$$R(x+\varepsilon) = \lambda(\varepsilon)R(x)(1-R(x)). \tag{2}$$

In a similar approach to multiple scales asymptotics, we treat the new 'slow' continuous variable $x$ as being independent of the 'fast' discrete variable $n$. We retain this independence by allowing our solution to be a function of $x$ and $\varepsilon$ (which is equivalent to allowing for fast variation in the discrete parameter).

We will obtain a formal solution in the general form of a so-called one-parameter transseries [29]:

$$R(x,\varepsilon;\sigma_0) = \sum_{m=0}^{\infty} \sigma_0^m \, \mathrm{e}^{-mA_0(x)/\varepsilon} \varepsilon^{m/2} \sum_{k=0}^{\infty} \varepsilon^k R_{m,k}(x). \tag{3}$$

This type of transseries is a formal expansion in both powers of the small parameter $\varepsilon$ and the monomial $\tau_0 = \sqrt{\varepsilon}\sigma_0 \, \mathrm{e}^{-A_0(x)/\varepsilon}$. In this formulation, we introduce a parameter $\sigma_0$ into the problem, which will be fixed by the initial conditions. While $\sigma_0$ is not small, it does act as an index for the small parameter $\tau_0$. This transseries expansion is valid in the regime where both $\varepsilon$ and $\tau_0$ are small. By treating $x$ as an continuum variable independent of $n$, we can remain in a regime in which $\tau_0$ is small, and the transseries expansion (3) is well-defined.

To study period-doubling bifurcations, we must consider behaviour that lies outside of this regime. We are interested in taking $n$ to be sufficiently large that we can detect the two-periodic solution that appears as a consequence of the first period-doubling bifurcation. This lies outside of the radius of convergence of the transseries summed over powers of $\tau_0$. In order to study the solution behaviour outside of its regime of validity, we apply the summation procedure known as transasymptotics.

We first rewrite the transseries (3) by changing the order of summation, giving

$$R(x,\epsilon) = \sum_{k=0}^{\infty} \varepsilon^k \sum_{m=0}^{\infty} \tau_0^m R_{m,k}(x) = \sum_{k=0}^{\infty} \varepsilon^k \Omega_k(\tau_0, x). \tag{4}$$

Here, we have defined the functions $\Omega_k(\tau, x)$ as the analytic continuations of the sum in powers of $\tau_0$. If we can find these functions, then we can evaluate the transseries solution in regions where $\tau_0$ is large (that is, regions in which $n$ is not small). This will allow us to extend the range of our solution outside of the regime of transseries validity.

We find $\Omega_k$ by rewriting the original logistic map to include the explicit dependence on $\tau_0(x,\varepsilon)$. Applying the reordered expression (3) to the resultant expression produces a set of differential equations for the functions $\Omega_k$ (nonlinear for $k = 0$, and linear for $k \geqslant 1$), which can be solved exactly. We will find that this procedure allows us to approximate the two-period solution very accurately using only the first few terms of the series (4). Importantly, the functions $\Omega_k$ do not become large when $\tau_0$ is large; they are instead finite in this limit, making the

sum in the transseries over powers of $\varepsilon$ either convergent (for the static case) or asymptotic (for the dynamic case).

The final step to the transasymptotic procedure is to determine the value of the free parameter $\sigma_0$. This is done by evaluating the transseries at $x = 0$ (corresponding to $n = 0$) and matching $\sigma$ expressed as a power series in $\varepsilon$ to the initial condition $R(0, \varepsilon)$.

*1.1.2. Studying higher-periodic behaviour using exponential weights.* We have described a systematic procedure which we will use to study the logistic map solution as two-period behaviour appears in the solution. A further aim of this study is to show that the preceding mathematical framework can be used to study the appearance of higher periodicity behaviour in the solution. From our transasymptotic analysis, we will determine that the origin of the two-periodic solution behaviour is a consequence of the exponential factor $\mathrm{e}^{-A_0(x)/\varepsilon}$, included in the parameter $\tau_0$, as it becomes large. By extension, we will show that further exponential weights in the transseries are responsible for subsequent period-doubling bifurcations.

When a transseries ansatz is used to solve a particular differential or difference equation, we generally obtain all possible values of the exponential weight $A_0(x)$ in straightforward fashion. However, the current problem displays behaviour not seen in previous studies on differential and difference equations. For example, in the static problem, we will find that the different exponential weights responsible for successive bifurcations are not active until certain critical values of $\varepsilon$ are reached (that are different for each exponential weight). Similar behaviour will be seen in the dynamic problem. Hence, more care is required in order to determine these weights.

Our procedure to obtain the subsequent exponential weights is as follows:

- We start with the transseries solution and take $x$ to be sufficiently large such that the two-periodic behaviour in the solution has stabilised; we will denote this expression as $R_0(x, \varepsilon)$. We may then expand $R_0$ for large $\tau_0$ and retain the leading order in this expansion.
- We then perturb the result by a new transseries $R_1$, such that

$$R(x, \varepsilon) = R_0(x, \varepsilon) + R_1(x, \varepsilon). \tag{5}$$

  Applying this ansatz to the original map produces a linear equation for $R_1$, which can be analysed in a similar fashion to the two-periodic bifurcation.
- We obtain a transseries expression for $R_1$, including the exponential weight $A_1(x, \varepsilon)$, exponential variable $\tau_1$, a new transseries index parameter $\sigma_1$, and the coefficients of the transseries expansion.
- In order to extend the regime in which the series is valid, we perform a transasymptotic summation of the system, allowing the solution to be extended into the region in which $\tau_1$ is not small.
- We finally determine the parameter $\sigma_1$ as a series in $\varepsilon$ to obtain the four-periodic solution behaviour[4].

We will use this process to obtain exponential weights that govern four-periodic behaviour in the logistic map solutions. Studying these exponential weights will explain why this behaviour did not appear in a straightforward small $\varepsilon$ analysis. The new exponential weight $A_1$ behaves differently on either side of a critical value $\varepsilon = \varepsilon_{1,\mathrm{c}}$, at which the exponential weight becomes infinitely large. This critical value separates two regimes of the second transseries. For

[4] The transseries parameters appearing in the augmented transseries are not free, and fixed by the initial condition and dependent on the previous parameter $\sigma_0$.

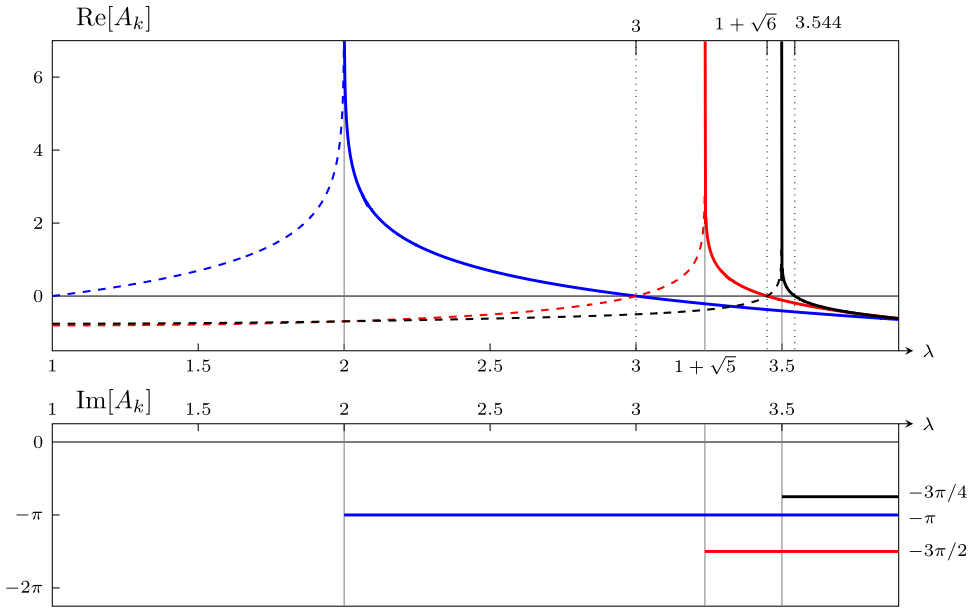


**Figure 2.** The first three exponential weights for the static logistic map, corresponding to two-periodic (blue), four-periodic (red), and eight-periodic (black) behaviour. The curves are dashed if the exponential lies on a different sheet, and unbroken if the exponential is on the solution sheet and contributes to the series behaviour. Critical values of $\lambda$ (and hence $\varepsilon$) are shown as a grey line, while threshold values are shown as a dotted line. For simplicity, the imaginary part of the weight is only shown in regimes where the weight is active.

$\varepsilon < \varepsilon_{1,\mathrm{c}}$ the exponential weight $A_1(x,\varepsilon)$ is on a separate sheet and does not contribute to the solution behaviour. Beyond the critical value, $A_1(x,\varepsilon)$ moves onto the primary sheet; the real part decreases from infinity, and this exponential contributes to the transseries behaviour.

In addition to explaining the appearance of higher-periodic effects in the solution, the exponential weights also explain why this bifurcation appears to be delayed. Upon moving onto the main solution sheet, the real part of $A_1$ is large, positive and real, corresponding to exponentially small values of $\tau_1$. As $\varepsilon$ increases past a threshold value $\varepsilon_{1,\mathrm{t}}$, the real part of $A_1$ changes sign. At this point, the effect of the transasymptotic summed functions $\Omega_k$ becomes significant, and periodic effects corresponding to $A_1$ become apparent in the solution.

The procedure described above can be used to obtain the further bifurcations by augmenting the transseries by extra components $R_j$ that have different exponential weights. Each of these weights will correspond to periodic behaviour with a different critical value $\varepsilon_{j,\mathrm{c}}$ at which the weight appears in the series, and a different threshold value $\varepsilon_{j,\mathrm{t}}$ at which it becomes comparable in size to the other exponentials present in the solution.

In figure 2, we illustrate the appearance of the first three exponential weights in the solution to the static logistic map, corresponding to two-, four-, and eight-periodic behaviour. In each case, we represent the weight as a dashed curve prior to the critical value of $\lambda$, corresponding to $\varepsilon_{j,\mathrm{c}}$, as it does not contribute to the series behaviour. Once this critical value is exceeded, the exponential moves onto the main sheet, but the contribution is exponentially small. When the real part of the weight changes sign at the threshold value, the behaviour associated with this weight becomes apparent in the solution.

We note from figure 2 that there are always regimes in $\lambda$, and hence $\varepsilon$, where the first $\tau_j$ parameters are large but the later ones are still suppressed, so the initial assumption that $\tau_0$ is large and $\tau_1$ is small was indeed valid.

We will follow this procedure throughout this paper to study periodic behaviour in the static logistic map in section 2, and delayed bifurcations in the dynamic logistic map in section 3. In sections 2.1 and 3.1 we formulate the transseries and obtain two-periodic solution behaviour. Four-periodic behaviour obtained in sections 2.2 and 3.2. In sections 2.3 and 3.3 these results are validated against numerical simulation and compared with earlier studies, and section 2.4 shows how eight-periodic behaviour may be found in the solution using these methods.

## 2. Static logistic equation

First we consider the static logistic equation, given by

$$y(n+1) = (3+\varepsilon)y(n)\,[1-y(n)]\,, \quad y(0) = 2/3. \tag{6}$$

We select $y(0) = 2/3$ as this is the stable solution for $\varepsilon = 0$. Hence any behaviour seen in the solution must be a consequence of the perturbation in the system. We will write the solution as a continuous transseries in terms of $\varepsilon > 0$. We first produce an asymptotic expansion in the limit $0 < \varepsilon \ll 1$ but as we shall see later, the transseries approach will be used to extend this result to produce an accurate approximation for $\varepsilon = \mathcal{O}(1)$. We will then show that this continuous transseries is capable of capturing discrete period-doubling effects seen in this system, and approximating higher periodicity behaviour for values of $\varepsilon$ that lead to two-, four- and even eight-periodic solutions.

In [42], the authors studied the asymptotic behaviour of this system for small $\varepsilon$ using multiple scales methods. This showed the manner in which the behaviour approached the two-periodic stable manifold associated with $\lambda > 3$. Using transseries methods, we can extend this approach to consider systems in which $\varepsilon$ is not asymptotically small, and demonstrate the manner in which the solution approaches the stable solution for higher periodicities.

In order to first determine the aperiodic and two-periodic solutions, we ignore the initial condition and solve (6) with the condition that $y(n+2) = y(n)$. This gives three unique solutions. One solution is aperiodic, and is given by

$$y(n) = \frac{2+\varepsilon}{3+\varepsilon}. \tag{7}$$

The remaining two solutions are two-periodic, and are given by

$$y(n) = \frac{4+\varepsilon \pm (-1)^n\sqrt{\varepsilon(4+\varepsilon)}}{2(3+\varepsilon)}. \tag{8}$$

For $\varepsilon > 0$, the aperiodic solution is unstable. For $0 < \varepsilon < \sqrt{6}-2$, the two-periodic solution is stable. If $\varepsilon$ exceeds $\sqrt{6}-2$, the two-periodic solution is unstable, and the stable solution to the system becomes four-periodic, and can be identified by solving $y(n+4) = y(n)$, however this solution cannot be expressed in closed form. Continuing to increase $\varepsilon$ leads to further increases in the periodicity of the stable solution, where the ratio of successive bifurcation intervals tends to Feigenbaum's constant [62]. The bifurcation intervals accumulate at $\lambda \approx 3.569\,94$, beyond which the solution demonstrates chaotic behaviour.

### *2.1. Two-periodic solution*

*2.1.1. Transseries ansatz.* We begin by applying a transseries ansatz, including a continuous variable $x$ and the small parameter $\varepsilon$. We set $x = \varepsilon n$, assuming for now $\varepsilon \ll 1$, and $R(x) = y(n)$ obeys

$$R(x+\varepsilon) = (3+\varepsilon)R(x)[1-R(x)], \qquad R(0) = 2/3. \tag{9}$$

We formulate an ansatz for the solution behaviour in terms of both $\varepsilon$ and a transseries parameter $\sigma_0$. The preliminary ansatz is given as a transseries described in section 1.1:

$$R(x,\varepsilon;\sigma_0) = \sum_{m=0}^{\infty} \sigma_0^m \, \mathrm{e}^{-mA(x)/\varepsilon} R_m(x,\varepsilon), \qquad R_m(x,\varepsilon) = \varepsilon^{\beta_m} \sum_{k=0}^{\infty} \varepsilon^k R_{m,k}(x), \tag{10}$$

where $\beta_m$ will be chosen such that $R_{m,0}$ takes a nonzero value. Applying this expression to (9) allows for the system to be matched in powers of $\sigma_0 \, \mathrm{e}^{-A(x)/\varepsilon}$, which is conveniently indexed by $\sigma_0$. At leading order, we find that the power series in (10) for $R_0$ is a convergent series, taking the value

$$R_0(x,\varepsilon) = \frac{2+\varepsilon}{3+\varepsilon}. \tag{11}$$

This expression gives the aperiodic manifold, which is stable for $1 < \lambda < 3$. For values of $\lambda$ greater than three, corresponding to positive $\varepsilon$, we expect to see additional periodic effects emerge from the transseries expression. Continuing to the next order in $\sigma_0 \, \mathrm{e}^{-A(x)/\varepsilon}$, we find that

$$\mathrm{e}^{-[A(x+\varepsilon)-A(x)]/\varepsilon} R_1(x+\varepsilon,\varepsilon) = -(1+\varepsilon)R_1(x,\varepsilon). \tag{12}$$

Expanding $R_1$ using (10) gives

$$\mathrm{e}^{-[A(x+\varepsilon)-A(x)]/\varepsilon} \sum_{k=0}^{\infty} \varepsilon^k R_{1,k}(x+\varepsilon) = -(1+\varepsilon) \sum_{k=0}^{\infty} \varepsilon^k R_{1,k}(x). \tag{13}$$

Expanding as a Taylor series in $\varepsilon$ gives $A(x+\varepsilon) = A(x) + \varepsilon A'(x) + \cdots$. Matching equal powers of $\varepsilon$ on both sides in (13) therefore requires $\exp(-A'(x)) = -1$, or

$$A(x) = (2p+1)\pi \mathrm{i} x, \quad p \in \mathbb{Z}. \tag{14}$$

The arbitrary constant in $A(x)$ may be absorbed into the transseries parameter $\sigma_0$, and is therefore set to be zero for convenience. The solution will only be evaluated for $n \in \mathbb{Z}$, which corresponds to $x/\varepsilon \in \mathbb{Z}$. The choice of $p$ has no effect at these values, and we therefore set $p = 0$ without loss of generality.

Using the expressions for $R_0$ in (11) and $A$ in (14) in (9) and tracking orders of $\sigma_0$, we obtain a recurrence relation for $R_m$:

$$(-1)^m R_m(x+\varepsilon,\varepsilon) = -(1+\varepsilon)R_m(x,\varepsilon) - (3+\varepsilon) \sum_{j=1}^{m-1} R_j(x,\varepsilon) R_{m-j}(x,\varepsilon), \tag{15}$$

for $m \geqslant 1$, where we take the convention that the summation term is zero when $m = 1$. It is straightforward to show by direct substitution that the solution to this recurrence takes the form

$$R_m(x,\varepsilon) = \mathrm{e}^{mx \, \log(1+\varepsilon)/\varepsilon} \overline{R}_m(\varepsilon), \qquad \overline{R}_m(\varepsilon) = \varepsilon^{\beta_m} \sum_{k=0}^{\infty} \varepsilon^k \overline{R}_{m,k}, \tag{16}$$

where the functions $\overline{R}_m(\varepsilon)$ can be computed directly. $\overline{R}_1(\varepsilon)$ may be chosen to be an arbitrary constant, which again can be absorbed into $\sigma_0$. For algebraic convenience, we can select $R_1(\varepsilon) = \varepsilon$. The subsequent terms may hence be obtained using the recursion (15), which gives the first few terms as

$$\begin{aligned}\overline{R}_2(\varepsilon) &= -\frac{(3+\varepsilon)\varepsilon^2}{(1+\varepsilon)(2+\varepsilon)}, \qquad \overline{R}_3(\varepsilon) = \frac{2(3+\varepsilon)^2\varepsilon^2}{(1+\varepsilon)^2(2+\varepsilon)^2},\\ \overline{R}_4(\varepsilon) &= -\frac{(3+\varepsilon)^3\,(\varepsilon-4)\,\varepsilon^3}{(1+\varepsilon)^3(2+\varepsilon)^3\left(1+\varepsilon+\varepsilon^2\right)}.\end{aligned} \tag{17}$$

By analysing the form of the recurrence solution, it is straightforward to determine $\beta_m$ in general, giving $\beta_m = (m+1)/2$ for $m$ odd, and $\beta_m = (m+2)/2$ for $m$ even. It can also be seen by direct calculation that

$$\overline{R}_{2m+1,0} = \frac{(-9)^m\Gamma\left(m+\frac{1}{2}\right)}{\sqrt{\pi}\Gamma\,(n+1)}, \qquad \overline{R}_{2m,0} = \frac{(-9)^m}{6}. \tag{18}$$

*2.1.2. Computing the terms in the resummed transseries.* The alternating behaviour of (18) combined with the general form of $R_m(x,\varepsilon)$ described in (16) suggests that the ansatz may be conveniently re-written to incorporate these elements explicitly. In particular, the fact that we have two different sub-series in (18) depending on the parity of $m$ suggests that we should split the series into odd and even powers of $m$. We therefore write the ansatz (10) as

$$\begin{aligned}R(x,\varepsilon;\sigma_0) = R_0(\varepsilon) &+ \sqrt{\varepsilon}\sum_{k=0}^{\infty}\varepsilon^k\sum_{m=0}^{\infty}\left(\sigma_0\sqrt{\varepsilon}\,\mathrm{e}^{-A(x)/\varepsilon + x\,\log(1+\varepsilon)/\varepsilon}\right)^{2m+1}\overline{R}_{2m+1,k}\\ &+ \varepsilon\sum_{k=0}^{\infty}\varepsilon^k\sum_{m=1}^{\infty}\left(\sigma_0\sqrt{\varepsilon}\,\mathrm{e}^{-A(x)/\varepsilon + x\,\log(1+\varepsilon)/\varepsilon}\right)^{2m}\overline{R}_{2m,k},\end{aligned} \tag{19}$$

where we have switched the order of summation, noting that the exponential terms are all of the same order in $\varepsilon$. Note that in the static case both sums in (19) are convergent. We define a new series parameter $\tau_0$, as well as odd and even power series in this parameter, such that

$$\begin{aligned}\tau_0(x,\varepsilon) &= \sigma_0\sqrt{\varepsilon}\,\mathrm{e}^{-A(x)/\varepsilon + x\,\log(1+\varepsilon)/\varepsilon}, \qquad \Omega_{\mathrm{o},k}(\tau_0) = \sum_{m=0}^{\infty}\tau_0^{2m+1}\overline{R}_{2m+1,k},\\ \Omega_{\mathrm{e},k}(\tau_0) &= \sum_{m=0}^{\infty}\tau_0^{2m}\overline{R}_{2m,k}.\end{aligned} \tag{20}$$

The transseries expression is now given by (the $x, \sigma_0$ dependence is encoded in $\tau_0$):

$$R(\tau_0,\varepsilon) = R_0(\varepsilon) + \sqrt{\varepsilon}\sum_{k=0}^{\infty}\varepsilon^k\Omega_{\mathrm{o},k}(\tau_0) + \varepsilon\sum_{k=0}^{\infty}\varepsilon^k\Omega_{\mathrm{e},k}(\tau_0). \tag{21}$$

We may apply this 'resummed' transseries to the logistic equation (9) and equate powers of $\varepsilon$ to obtain expressions for $\Omega_{\mathrm{o},k}$ and $\Omega_{\mathrm{e},k}$. This process is somewhat technical, and is shown explicitly in appendix A. Equating terms of order $\varepsilon$ and $\varepsilon^{3/2}$ respectively gives

$$\Omega_{\mathrm{e},0} = -\frac{3}{2}(\Omega_{\mathrm{o},0})^2, \qquad \tau_0\frac{\mathrm{d}\Omega_{\mathrm{o},0}}{\mathrm{d}\tau_0} = \Omega_{\mathrm{o},0} - 9(\Omega_{\mathrm{o},0})^3. \tag{22}$$

Solving the ordinary differential equation gives $\Omega_{\mathrm{o},0}(\tau_0) = \pm\tau_0(C + 9\tau_0^2)^{-1/2}$. The sign and constant may be chosen arbitrarily, as this choice again can be absorbed into $\sigma_0$, which is yet to be determined. In order to maintain consistency with (17), we select the positive sign and $C = 1$, giving

$$\Omega_{\mathrm{o},0}(\tau_0) = \frac{\tau_0}{\sqrt{1+9\tau_0^2}}, \qquad \Omega_{\mathrm{e},0}(\tau_0) = -\frac{3}{2}\frac{\tau_0^2}{(1+9\tau_0^2)}. \tag{23}$$

Continuing this process and equating terms of order $\varepsilon^2$ and $\varepsilon^{5/2}$ respectively gives

$$\Omega_{\mathrm{e},1} = \frac{\tau_0^2\left(14-9\tau_0^2\right)}{8(1+9\tau_0^2)^2} - 3\Omega_{\mathrm{o},0}\Omega_{\mathrm{o},1}, \qquad \tau_0\frac{\mathrm{d}\Omega_{\mathrm{o},1}}{\mathrm{d}\tau_0} = \frac{1-18\tau_0^2}{1+9\tau_0^2}\Omega_{\mathrm{o},1} + \frac{3\tau_0^2(28-45\tau_0^2)}{4\left(1+9\tau_0^2\right)^{5/2}}. \tag{24}$$

Solving these equations gives

$$\begin{aligned}\Omega_{\mathrm{o},1}(\tau_0) &= -\frac{\tau_0(45\tau_0^2 - 33\,\log(1+9\tau_0^2))}{24(1+9\tau_0^2)^{3/2}},\\ \Omega_{\mathrm{e},1}(\tau_0) &= \frac{\tau_0^2\left(14+36\tau_0^2-33\,\log\left(1+9\tau_0^2\right)\right)}{8(1+9\tau_0^2)^2},\end{aligned} \tag{25}$$

where yet again the arbitrary constant of integration can be chosen arbitrarily with the choice being absorbed into $\sigma_0$, and was therefore selected in order to maintain consistency with (17). In principle, this process can be continued to higher transasymptotic order indefinitely by matching at higher orders of $\varepsilon$.

We can compare these expressions to the multiple scales expansion obtained in [42]. A straightforward comparison shows that the expression $\Omega_{\mathrm{o},1}$ gives the first correction to the composite expansion, denoted $P(s)$, from [42]. The expression for $P(s)$ contains an exponential multiplier $\mathrm{e}^s$, which corresponds to the exponential scaling in $\tau_0$. This confirms that the resummed transseries identifies the region in which the power series expression breaks down, and allows for the expansion to be continued past this region even without the use of matched asymptotic expansions.

*2.1.3. Initial value problem.* In order to complete the approximation, we must determine the value of $\sigma_0$ using the initial condition in (9), which requires that $R(x=0,\varepsilon;\sigma_0) = 2/3$. Noting that $\tau_0(x=0,\varepsilon) = \sqrt{\varepsilon}\sigma_0$, this corresponds to solving

$$R_0(\varepsilon) + \sqrt{\varepsilon}(\Omega_{\mathrm{o},0}(\sigma_0\sqrt{\varepsilon}) + \varepsilon\Omega_{\mathrm{o},1}(\sigma_0\sqrt{\varepsilon})) + \varepsilon(\Omega_{\mathrm{e},0}(\sigma_0\sqrt{\varepsilon}) + \varepsilon\Omega_{\mathrm{e},1}(\sigma_0\sqrt{\varepsilon})) + \mathcal{O}(\varepsilon^4) = \frac{2}{3}. \tag{26}$$

By expanding $\sigma_0$ as a power series in $\varepsilon$ such that

$$\sigma_0(\varepsilon) = \sum_{j=0}^{\infty}\varepsilon^j\sigma_{0,j}. \tag{27}$$

Matching powers of $\varepsilon$ in (26) now gives

$$\sigma_{0,0} = -\frac{1}{9}, \qquad \sigma_{0,1} = \frac{4}{81}, \qquad \sigma_{0,2} = -\frac{19}{648}. \tag{28}$$

This process may be continued as $\Omega_{\mathrm{o},k}$ and $\Omega_{\mathrm{e},k}$ are computed for higher values of $k$, giving the increasingly complete expression for the two-periodic behaviour. While we expect (27) to be convergent, we have not demonstrated this fact; nonetheless, this method for solving for the coefficients $\sigma_{0,j}$ is valid irrespective of whether this is a convergent or divergent asymptotic series.

### 2.2. Four-periodic solution

*2.2.1. Transseries ansatz.* To obtain the four-periodic solution requires an adaptation of the previous process. We now take a four-periodic perturbation about the two-periodic solution obtained in (26). This allows us to form a transseries that can be used to capture solutions which tend to a four-periodic stable manifold. In [42], this would have required solving a challenging multiple scales problem, as the asymptotic solution obtained therein is only valid for small $\varepsilon$. Using the transseries approach, we obtain a significant more general result.

We write the solution as a perturbation around the aperiodic behaviour and the two-periodic behaviour captured by the transseries expression (21), in terms of the variable $\tau_0$, here written as $\hat{R}(\tau_0, \varepsilon)$.

$$R(x,\varepsilon) = R_0(\varepsilon) + \sqrt{\varepsilon}\sum_{k=0}^{\infty}\varepsilon^k\Omega_{\mathrm{o},k}(\tau) + \varepsilon\sum_{k=0}^{\infty}\varepsilon^k\Omega_{\mathrm{e},k}(\tau) + S(x,\varepsilon) = \hat{R}(x,\varepsilon) + S(x,\varepsilon). \tag{29}$$

We will then show that this perturbation starts contributing for values of $\varepsilon$ large enough. We can see by direct substitution into (9) that

$$S(x+\varepsilon,\varepsilon) = (3+\varepsilon)(1 - 2\hat{R}(\tau_0,\varepsilon) - S(x,\varepsilon))S(x,\varepsilon). \tag{30}$$

In order to identify the correct scaling for $S(x)$, we note the form of the two-periodic manifold, given in (8). We represent the two-periodic behaviour in terms of the continuous variable $x$ by writing $(-1)^n$ as $\alpha = \ \mathrm{sign}(\cos(\pi x/\varepsilon))$, such that

$$\hat{R}(\tau_0,\varepsilon) = \frac{4+\varepsilon-\alpha\sqrt{\varepsilon(4+\varepsilon)}}{2(3+\varepsilon)} + \mathcal{O}(\tau_0^{-1}) \quad \text{as } x\to\infty, \tag{31}$$

where the asymptotic order of this expression can be obtained by rewriting (26) in powers of $\tau_0^{-1}$ and equating terms. We may now follow similar methods to the two-periodic case, and formulate an ansatz for the solution in terms of $\varepsilon$ and a new transseries parameter, denoted $\sigma_1$. Motivated by (16), we choose the ansatz

$$S(x,\varepsilon) = \sum_{m=1}^{\infty}\sigma_1^m\,\mathrm{e}^{-mB(x,\varepsilon)/\varepsilon}S_m(\varepsilon), \tag{32}$$

noting that we now allow an $\varepsilon$ dependence on the exponential scale. The exponential scaling $B(x,\varepsilon)$ may then be determined by considering the large-$x$ behaviour. This is convenient, as we have the form for $R(x)$ in this limit, given in (31), and we know from the asymptotic order of this expression that the solution approaches this limit exponentially as $x$ becomes large. Using (31) in (30) and matching powers of $\varepsilon$ in an identical fashion to (13) gives

$$\frac{\partial}{\partial x}B(x,\varepsilon) = -\pi\mathrm{i} - \log\left(1-\alpha\sqrt{\varepsilon(4+\varepsilon)}\right). \tag{33}$$

This may be solved to give

$$B(x,\varepsilon) = f(\varepsilon)x - \varepsilon g(x,\varepsilon), \tag{34}$$

where

$$f(\varepsilon) = -\frac{1}{2}\log(1-\varepsilon(4+\varepsilon)) - \pi\mathrm{i}, \tag{35}$$

and $g(x,\varepsilon)$ is a bounded function that vanishes for $x = \varepsilon n$ for $n \in \mathbb{Z}$, given by

$$g(x,\varepsilon) = \alpha\left(\frac{x}{2\varepsilon} - \frac{1}{2}\left\lfloor\frac{x}{\varepsilon} + \frac{1}{2}\right\rfloor\right)\log\left(\frac{1-\sqrt{\varepsilon(4+\varepsilon)}}{1+\sqrt{\varepsilon(4+\varepsilon)}}\right). \tag{36}$$

As $g(n\varepsilon,\varepsilon) = 0$ for $n \in \mathbb{Z}$, this expression could be ignored and the result will still give the correct value of $B(x,\varepsilon)$, and hence the correct exponential scaling, on $x = \varepsilon n$. This therefore suggests that we can capture the four-periodic solution by defining a new variable $\tau_1$, such that

$$\tau_1(x,\varepsilon) = \sigma_1\sqrt{\varepsilon}\,\mathrm{e}^{-B(x,\varepsilon)/\varepsilon}. \tag{37}$$

In subsequent analysis, it will be useful to have a convenient expression for the value of $\tau_1$ at $x+\varepsilon$ and $x+2\varepsilon$. Through direct substitution, we find that

$$\tau_1(x+\varepsilon,\varepsilon) = -\mathrm{i}(\varepsilon(4+\varepsilon)-1)^{1/2}\,\mathrm{e}^{-2g(x,\varepsilon)}\tau_1(x,\varepsilon), \tag{38}$$

$$\tau_1(x+2\varepsilon,\varepsilon) = -(\varepsilon(4+\varepsilon)-1)\tau_1(x,\varepsilon). \tag{39}$$

*2.2.2. Exponential weights.* The form of $B(x,\varepsilon)$ provides insight into the behaviour of the solution as $\varepsilon$ increases outside of the range of validity of the original small-$\varepsilon$ transseries. The behaviour of this term is shown in figure 3, which identifies three distinct ranges of $\varepsilon$ which must be considered separately.

From the form of (37), we see that $B(x,\varepsilon)$ is the exponential controlling factor for $S$, and therefore determines how this series will contribute as $x$ grows. If $\mathrm{Re}[B] > 0$, corresponding to $\mathrm{Re}[f(\varepsilon)] > 0$, the exponential contribution will decay as $x$ grows, while if $\mathrm{Re}[B] < 0$, corresponding to $\mathrm{Re}[f(\varepsilon)] < 0$, the exponential part will grow and become the most significant contribution for large $x$.

This change in sign occurs at $\varepsilon = -2+\sqrt{6}$. At this point, $\mathrm{Re}[f(\varepsilon)]$ becomes negative, and the exponentials in (32) therefore grow as $x$ becomes large, rather than decaying. This means that in region ③ the $S$ term is no longer a small decaying perturbation around $\hat{R}$, but rather plays a significant role in the limiting behaviour as $x \to \infty$. If $S$ is ignored, this behaviour is not captured in the transseries, and the resultant expression for $R$ is an inaccurate description of the solution behaviour.

We note that $\mathrm{Im}[f(\varepsilon)] = -3\pi/2$ for $\varepsilon > -2+\sqrt{5}$. This has the effect of making $\tau_1^m$ four-periodic in $m \in \mathbb{Z}^+$, due to having a factor of $-\mathrm{i}$, rather than the two-periodic behaviour associated with a factor of $-1$. Hence, this exponential behaviour represented by $B(x,\varepsilon)$ corresponds to four-periodic effects in the solution.

In order to include this behaviour in the transseries expression, we cannot simply expand the solution about $\varepsilon = 0$. We must instead expand $S$ about some point $\varepsilon_0$ such that the four-periodic behaviour is present in the expansion. This requirement suggests that $\varepsilon_0 = -2+\sqrt{6}$ is a sensible choice, as four-periodic effects are apparent in the solution at this value.

Finally, we must consider the region in which the series terms obtained by expanding about $\varepsilon_0$ are valid. If we examine the behaviour of $B(x,\varepsilon)$ for $\varepsilon > \varepsilon_0$, we see that the real part of $f(\varepsilon)$ becomes infinite as $\varepsilon \to -2+\sqrt{5}$. This corresponds to the exponentials disappearing, as every exponential term tends to zero. The series expansion about $\varepsilon_0$ is not valid for $\varepsilon$ smaller than this value. Consequently, region ② contains exponentially small four-periodic behaviour,

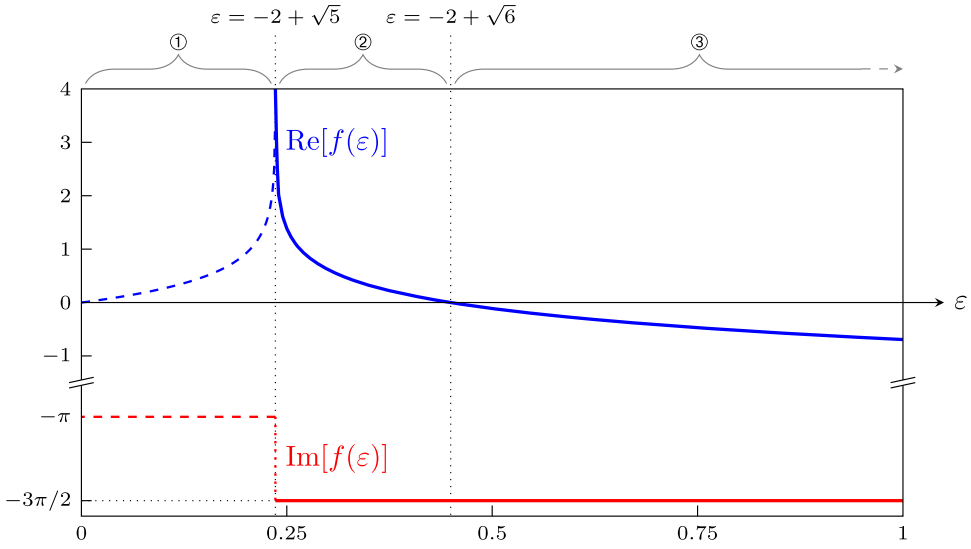


**Figure 3.** This figure shows the real and imaginary parts of $f(\varepsilon) = -\frac{1}{2}\log(1-\varepsilon(4+\varepsilon)) - \pi\mathrm{i}$, where the exponential weight $B(x)$ is given in (34). If $\mathrm{Re}[f(\varepsilon)] > 0$, the four-periodic exponential contribution is exponentially small in $\varepsilon$, while if $\mathrm{Re}[f(\varepsilon)] < 0$, the contribution is large, and must be incorporated into any approximation in order to accurately describe the system behaviour. In parameter regime ①, this exponential contribution is not present in the transseries, and is therefore denoted as a dashed curve. In regime ②, the four-periodic exponential terms appear, but are exponentially small. In regime ③, the exponential contributions become large, and four-periodic behaviour becomes apparent in the solution. The four-periodicity of the solution arises due to $\mathrm{Im}[f(\varepsilon)]$. This represents a multiplicative factor in $B(x)$ of $-\mathrm{i}$, corresponding to four-periodic behaviour in the exponential term.

while no such behaviour exists in region ①. In figure 3 we have represented $f(\varepsilon)$ in region ① as a dashed curve, to indicate that it does not have any effect on the transseries.

Consequently, simply by studying $B(x,\varepsilon)$, we are able to describe the onset of four-periodicity in the solution. In region ①, there are no four-periodic effects present. In region ②, there are four-periodic effects caused by the appearance of new exponential terms, but they are exponentially subdominant compared to the two-periodic behaviour. In region ③, these effects grow to become the most significant effect in the solution behaviour. Note that the switching of the four-period exponentials is independent of the initial data, the latter only determines how quickly they grow to dominate the solution. For higher values of $\varepsilon$, there must be values for which higher-periodicity behaviour appears. We discuss the onset of eight-periodic behaviour in section 2.4.

Finally, we note that the change in exponential contribution has a parallel with a Borel transform approach to asymptotic expansions. Borel transforms encode the different exponential weights of an asymptotic series as singularities in a complex domain known as the 'Borel plane'. There, a change in the number of exponential contributions corresponds to singularities moving across a branch cut onto a different Riemann sheet of the Borel plane, giving rise to behaviour known as the 'Stokes phenomenon' [11] as the number of exponential contributions in an asymptotic series abruptly changes. A similar, but not identical, behaviour occurs in this system at $\varepsilon = -2+\sqrt{5}$, where $\mathrm{Re}[f(\varepsilon)]$ becomes infinite and $\mathrm{Im}[f(\varepsilon)]$ changes instantaneously, corresponding to a branch point in the $f$-plane. As the power series in (10) is a

convergent series, this is not a strict example of the Stokes phenomenon, despite the appearance of new exponential contributions. The appearance of these exponentials here is due to the nonlinearity of the problem. In more complicated problems with divergent asymptotic power series, such as the dynamic logistic map considered in section 3, the Stokes phenomenon is encoded in the form of the late-order series terms, and can be understood by studying the behaviour of the exponential weights when encoded in the Borel plane. For more information on Borel transform methods, and their links to transseries and transasymptotic summations, see [2, 14, 16, 45, 55, 56].

*2.2.3. Computing the terms in the resummed transseries.* Writing an appropriate form for the four-periodic ansatz is slightly more involved than in the two-periodic case, given in (19). Recall from section 2.2.2 that the significant change in the behaviour of the exponential contribution occurs for values of $\varepsilon$ greater than $\varepsilon_0 = -2 + \sqrt{6}$. We therefore define a new series variable $\sqrt{6}\eta = \varepsilon - \varepsilon_0$, where the $\sqrt{6}$ term is included for subsequent algebraic convenience.

In analogous fashion to (21), we again divide the ansatz up into separate power series. In the two-periodic case, it was clear from the form of the previously calculated terms that splitting the odd and even powers of $\tau_0$ would capture the discrete variation effectively. From the analysis in section 2.2.2, we determine that the power series for the four-periodic solution should instead be split into four parts, such that

$$\begin{aligned} S(\tau_1,\eta) = {} & \sqrt{\eta}\sum_{k=0}^{\infty}\eta^k\sum_{m=0}^{\infty}\tau_1^{4m+1}S_{4m+1,k} + \eta\sum_{k=0}^{\infty}\eta^k\sum_{m=0}^{\infty}\tau_1^{4m+2}S_{4m+2,k} \\ & + \sqrt{\eta}\sum_{k=0}^{\infty}\eta^k\sum_{m=0}^{\infty}\tau_1^{4m+3}S_{4m+3,k} + \eta\sum_{k=0}^{\infty}\eta^k\sum_{m=0}^{\infty}\tau_1^{4m+4}S_{4m+4,k}. \end{aligned} \tag{40}$$

Consequently, we now write each split power series as functions $\Theta_{j,k}$, $j = 1, 2, 3, 4$, giving

$$S(\tau_1,\eta) = \sqrt{\eta}\sum_{k=0}^{\infty}\eta^k\Theta_{1,k}(\tau_1) + \eta\sum_{k=0}^{\infty}\eta^k\Theta_{2,k}(\tau_1) + \sqrt{\eta}\sum_{k=0}^{\infty}\eta^k\Theta_{3,k}(\tau_1) + \eta\sum_{k=0}^{\infty}\eta^k\Theta_{4,k}(\tau_1). \tag{41}$$

Noting that each series consists only of powers $\tau_1^m$ with the same $m \bmod 4$, and comparing this with the expression for $\tau_1$ in (37) indicates that the functions $\Theta_{j,k}$ for $j = 1, \ldots, 4$ must have the symmetries

$$\Theta_{1,k}(-\mathrm{i}\tau_1) = -\mathrm{i}\Theta_{1,k}(\tau_1), \qquad \Theta_{2,k}(-\mathrm{i}\tau_1) = -\Theta_{2,k}(\tau_1), \tag{42}$$

$$\Theta_{3,k}(-\mathrm{i}\tau_1) = \mathrm{i}\Theta_{3,k}(\tau_1), \qquad \Theta_{4,k}(-\mathrm{i}\tau_1) = \Theta_{4,k}(\tau_1). \tag{43}$$

At this stage, it might be expected that we should express the governing equation (30) in terms of $\eta$, and perform an expansion in this variable; however, a comparison of the terms in (38) and (39) suggests that iterating the map once leads to a simplification. Writing the $x$ dependence explicitly, the equation becomes:

$$\begin{aligned} S(x+2\varepsilon,\varepsilon) = {} & (3+\varepsilon)^2(1-2\widehat{R}(x,\varepsilon) - S(x,\varepsilon))S(x,\varepsilon) \\ & \times \left[1 - 2\widehat{R}(x+\varepsilon,\varepsilon) - (3+\varepsilon)(1-2\widehat{R}(x,\varepsilon) - S(x,\varepsilon))S(x,\varepsilon)\right]. \end{aligned} \tag{44}$$

This expression does not contain any $S(x+\varepsilon,\varepsilon)$ terms, and instead only contains the double iteration term, $S(x+2\varepsilon,\varepsilon)$. This is convenient, as the expression for $\tau_1(x+2\varepsilon,\varepsilon)$ is substantially simpler than $\tau_1(x+\varepsilon,\varepsilon)$, as it does not contain $g(x,\varepsilon)$. This simplifies significantly the subsequent analysis.

Expressing the left-hand term in (44) in terms of $\tau_1$ and $\eta$ gives

$$S(x+2\varepsilon,\varepsilon) = S(-(\varepsilon(4+\varepsilon)-1)\tau_1,\varepsilon) = S(-(1+12\eta+6\eta^2)\tau_1,\eta). \tag{45}$$

Rewriting (44) in terms of $\tau_1$ and $\eta$ therefore gives

$$\begin{aligned} S(-(1+12\eta+6\eta^2)\tau_1,\eta) = S(\tau_1,\eta)\left(1-\alpha\sqrt{2+12\eta+6\eta^2}+(1+\sqrt{6}(1+\eta))S(\tau_1,\eta)\right) \\ \times\left(1+\alpha\sqrt{2+12\eta+6\eta^2}-(1+\sqrt{6}(1+\eta))^2S(\tau_1,\eta)^2\right. \\ \left.-S(\tau_1,\eta)(1+\sqrt{6}(1+\eta))\left(1-\alpha\sqrt{2+12\eta+6\eta^2}\right)\right). \end{aligned} \tag{46}$$

Analogously to the analysis of the two-periodic case in appendix A, the next step is to expand this expression as a power series in $\eta$, and apply the series expression for $S(\tau_1,\eta)$ given in (40). Matching powers of $\eta^{j/2}$ for $j=1,\ldots 4$ produces a system of four equations—two of these equations are algebraic, and two are nonlinear ordinary differential equations in $\tau_1$. We omit the details of this step here, as it requires only algebraic manipulations, and the intermediate mathematical expressions are quite lengthy. These four equations may be simplified using the symmetry relations in (42) and (43), resulting in the following system of equations

$$\Theta_{4,0}(\tau_1) = 2a\Theta_{1,0}(\tau_1)\Theta_{3,0}(\tau_1), \tag{47}$$

$$\Theta_{2,0}(\tau_1) = a\Theta_{1,0}(\tau_1)^2 + a\Theta_{3,0}(\tau_1)^3, \tag{48}$$

$$\tau_1\Theta'_{1,0}(\tau_1) = \Theta_{1,0}(\tau_1) - b(\Theta_{3,0}(\tau_1)^3 + 3\Theta_{1,0}(\tau_1)^2\Theta_{3,0}(\tau_1)), \tag{49}$$

$$\tau_1\Theta'_{3,0}(\tau_1) = \Theta_{3,0}(\tau_1) - b(\Theta_{1,0}(\tau_1)^3 + 3\Theta_{3,0}(\tau_1)^2\Theta_{1,0}(\tau_1)), \tag{50}$$

where

$$a = \frac{1}{2}\left(2+2\sqrt{6}-3\alpha(\sqrt{2}+2\sqrt{3})\right), \qquad b = \frac{5}{6}\left(14+4\sqrt{6}-\alpha(7\sqrt{2}+4\sqrt{3})\right). \tag{51}$$

By substituting the power series (40) into the governing equation (46), it can be seen at leading order as $\eta\to 0$ and $\tau_1\to 0$ that $S_{1,0} = -S_{3,0}$, providing one initial condition for the system (47)–(50). The second initial condition may be chosen arbitrarily, as this choice may be absorbed into the expression for $\sigma_1$, in the same manner as the constant $C$ in (22). For algebraic convenience, and without loss of generality, we select $S_{1,0}=1$. These conditions are sufficient to uniquely solve (47)–(50). The solution to this system is given by

$$\Theta_{1,0}(\tau_1) = \frac{\alpha\tau_1}{\sqrt{2-2b^2\tau_1^4}}\sqrt{1+\sqrt{1-b^2\tau_1^4}}, \tag{52}$$

$$\Theta_{2,0}(\tau_1) = -\frac{a\tau_1^2}{1-b^2\tau_1^4}, \tag{53}$$

$$\Theta_{3,0}(\tau_1) = -\frac{\alpha b\tau_1^3}{\sqrt{2-2b^2\tau_1^4}}\left(\sqrt{1+\sqrt{1-b^2\tau_1^4}}\right)^{-1}, \tag{54}$$

$$\Theta_{4,0}(\tau_1) = \frac{ab\tau_1^4}{1 - b^2\tau_1^4}. \tag{55}$$

In principle, we can match the expansion of (46) at higher powers of $\eta$ in order to obtain $\Theta_{j,k}$ for $j = 1, \ldots 4$ with $k > 0$. For the purposes of this example, however, the first four terms of the series will produce a useful approximation for the solution behaviour.

The final step is to determine the behaviour of the transseries parameter $\sigma_1$. This is slightly more complicated than in the two-periodic problem, as we must incorporate the behaviour of $\hat{R}(x, \varepsilon)$ into the calculations. We include the details of this process in appendix B, where we show that

$$\begin{aligned}\sigma_1 = &-\frac{1}{50}\left(3\sqrt{2} - 16\sqrt{3} - 7\sqrt{6} + 12\right) \\ &+ \frac{\eta}{500}\left(297\sqrt{2} - 709\sqrt{3} - 189\sqrt{2} + 399\right) + \mathcal{O}(\eta^2).\end{aligned} \tag{56}$$

We have now determined enough transseries terms to accurately approximate the solution behaviour in the four-periodic regime.

### 2.3. Error comparison

As a consequence of the preceding analysis, we are able to derive an approximation for the solution to the logistic equation in the two-periodic and four-periodic parameter regimes, which we denote as $R_{2,\mathrm{app}}(x)$ and $R_{4,\mathrm{app}}(x)$ respectively. Combining (20), (21), (23), (25), and (28), we find that in the two-periodic parameter regime

$$R(x) \approx R_{2,\mathrm{app}}(x) = \frac{2+\varepsilon}{3+\varepsilon} + \varepsilon^{1/2}\Omega_{\mathrm{o},0}(\tau_0) + \varepsilon\Omega_{\mathrm{e},0}(\tau_0) + \varepsilon^{3/2}\Omega_{\mathrm{o},1}(\tau_0) + \varepsilon^2\Omega_{\mathrm{e},1}(\tau_0), \tag{57}$$

where $\tau_0$ and $\sigma_0$ are approximated as

$$\tau_0 = \sigma_0\varepsilon^{1/2}\,\mathrm{e}^{-x(\pi\mathrm{i}+\log(1+\varepsilon))/\varepsilon}, \qquad \sigma_0 \approx -\frac{1}{9} + \frac{4\varepsilon}{81} - \frac{19\varepsilon^2}{648}. \tag{58}$$

A comparison of the exact solution against the approximation is shown for $\varepsilon = 0.05$ in figure 4(a). The exact solution is shown as red circles, while the approximation is shown as blue dots. The two curves are visually indistinguishable. The approximation error is shown in figure 4(c). It is clear from this figure that the error has a peak at the end of the transition region, just before the solution settles into the stable two-periodic behaviour.

In the four-periodic parameter regime $\varepsilon > -2 + \sqrt{6}$, the approximated transseries is given combining the expressions in (37), (52)–(56), and the previous approximation (57), to give

$$R(x) \approx R_{4,\mathrm{app}}(x) = R_{2,\mathrm{app}}(x) + \sqrt{\eta}(\Theta_{1,0}(\tau_1) + \Theta_{3,0}(\tau_1)) + \eta(\Theta_{2,0}(\tau_1) + \Theta_{4,0}(\tau_1)), \tag{59}$$

where $\tau_1$ and $\sigma_1$ are approximated as

$$\tau_1 = \sigma_1\varepsilon^{1/2}\,\mathrm{e}^{x(\log(1-\varepsilon(4+\varepsilon))/2+\pi\mathrm{i})/\varepsilon}, \tag{60}$$

and

$$\sigma_1 \approx -\frac{1}{50}\left(3\sqrt{2} - 16\sqrt{3} - 7\sqrt{6} + 12\right) + \frac{\eta}{500}\left(297\sqrt{2} - 709\sqrt{3} - 189\sqrt{2} + 399\right). \tag{61}$$

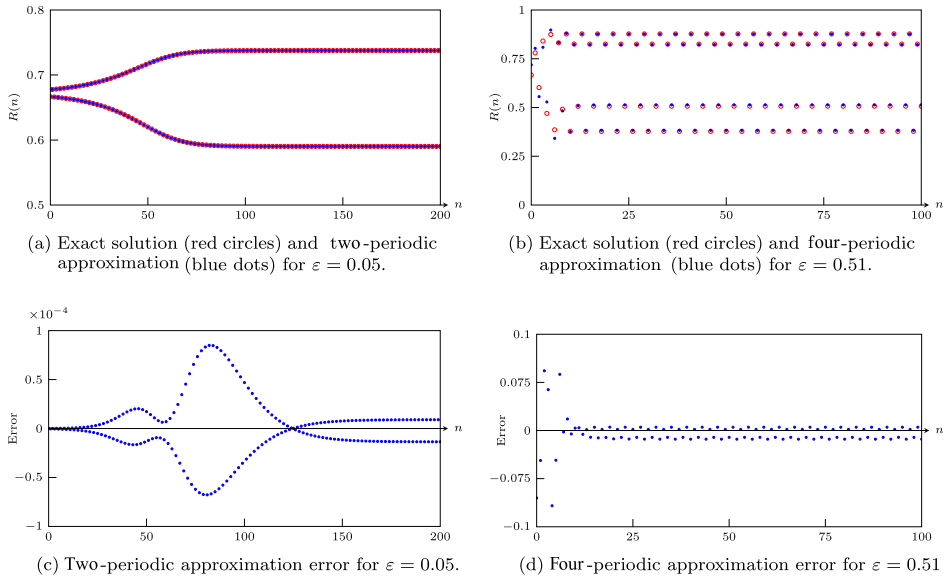


(a) Exact solution (red circles) and two-periodic approximation (blue dots) for $\varepsilon = 0.05$.

(b) Exact solution (red circles) and four-periodic approximation (blue dots) for $\varepsilon = 0.51$.

(c) Two-periodic approximation error for $\varepsilon = 0.05$.

(d) Four-periodic approximation error for $\varepsilon = 0.51$

**Figure 4.** The plot in (a) compares the two-periodic approximation $R_{2,\text{app}}$, from (57), against the exact solution for $\varepsilon = 0.05$. The plot in (b) compares the four-periodic approximation $R_{4,\text{app}}$, from (59), against the exact solution for $\varepsilon = 0.51$, or $\sqrt{6}\eta \approx 0.0605$. The approximation errors, given by the difference between the exact solution $R(x)$ and the approximations are shown in (c) and (d). The two-periodic approximation has maximum error in the region just before reaching the two-periodic steady solution. The four-periodic approximation has maximum error in the initial region; this is to be expected, as the initial condition was obtained directly from the two-periodic solution, and is not expected to be highly accurate in the four-periodic regime.

Note that we do not include the term containing $g(x, \varepsilon)$ in $B(x, \varepsilon)$ from (34). This term disappears for integer values of $n$, and therefore can be omitted at this stage without altering the approximation.

In figure 5(a), we show the approximation error for a range of values of $\varepsilon$, where the error is measured as the maximum difference between the exact solution and the transseries approximation, shown as a blue curve. This error measure was chosen to allow for direct comparison with equivalent results from [42], which are shown as a red curve. The transseries approximation is more accurate than the multiple scales approximation in this parameter regime, and the error decays faster in the limit that $\varepsilon \to 0$. The reason for this behaviour is that the transseries approach allowed for higher-order exponential corrections to be easily computed and retained. The maximum approximation error occurs at the end of the transition region between aperiodic and two-periodic behaviour, where the exponential contributions contribute significantly to the solution behaviour. Computing these exponential corrections using multiple scales methods would be an algebraically significantly more demanding task, requiring matched asymptotic expansions to be applied at higher orders of the expansion.

### *2.4. Eight-periodic solution*

We may continue this process to understand the emergence of the next period doubling bifurcation. While we will not include a full explicit, algebraic analysis here, we will show that the

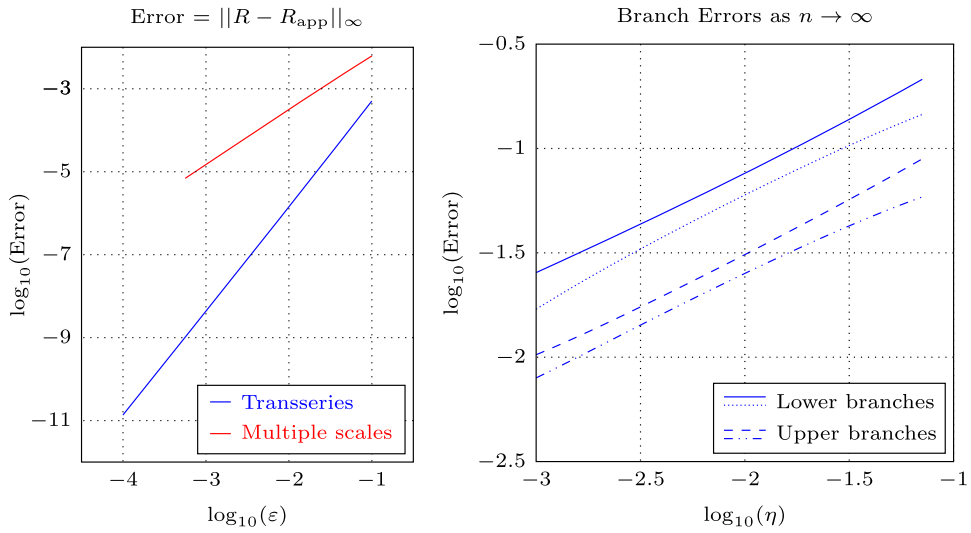


(a) Error for Two-Periodic Approximation (b) Error for Four-Periodic Approximation

**Figure 5.** The plot in (a) shows the resummed transseries approximation error in blue, corresponding to the maximum difference between the approximated and exact value. This measure of the error was chosen to be consistent with the error measure provided in [42]; this error is shown as a red curve. Due to the ease with which the transseries method captures higher-order exponential behaviour, which plays an important role in the transition region between aperiodic and two-periodic behaviour, it outperforms the multiple scales approximation. In (b), we show the error of the four solution branches as $n \to \infty$, approximated by taking $|R - R_{4,\text{app}}|$ on each of the four branches for a value of $n$ sufficiently large that the error is not visibly changing. For each of the four branches, the error decreases as $\eta \to 0$, as would be expected. Figures (a) and (b) were generated by computing the approximation error at $10^4$ points distributed evenly across the parameter range.

exponential factor can be used to identify the appearance of eight-periodic stable solutions as $\varepsilon$ is increased further.

The method from section 2.2 can be applied again in order to obtain approximations for solutions with even higher periodicity. We can now write the next term in the transseries such that $R(x,\varepsilon) = \hat{R}(x,\varepsilon) + S(x,\varepsilon) + T(x,\varepsilon)$. The quantity $T(x,\varepsilon)$ is defined in terms of a new transseries parameter $\sigma_2$ to be

$$T(x,\varepsilon;\sigma_2) = \sum_{m=1}^{\infty} \sigma_2^m \, \mathrm{e}^{-mF(x,\varepsilon)/\varepsilon} T_m(\varepsilon). \tag{62}$$

The transseries terms $\hat{R} + S$ capture the four-periodic solution behaviour, and therefore must tend to the four-periodic solution in the limit that $\tau_0$ and $\tau_1$ become large. We denote this solution as $R_4(\varepsilon)$. Hence, we apply the expression $R(x,\varepsilon) = R_4(\varepsilon) + T(x,\varepsilon)$ to the governing equation (9) and find an expression for the exponential weights, in similar fashion to the process for obtaining (14) or (33).

The exponential weights may again be written in the form $F(x,\varepsilon) = f(\varepsilon)x + \varepsilon g(x,\varepsilon)$, where $g$ disappears on $n \in \mathbb{Z}$. The behaviour of $f(\varepsilon)$ is illustrated in figure 6. A very similar set of inferences may be drawn from this image as for figure 3. In region, the eight-periodic behaviour

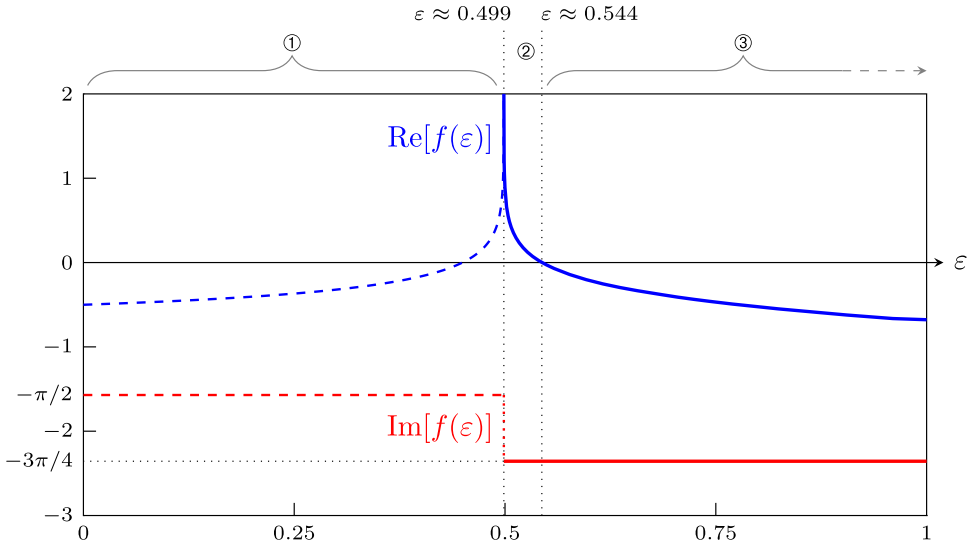


**Figure 6.** This figure shows the real and imaginary parts of $f(\varepsilon)$, where $F(x,\varepsilon) = f(\varepsilon)x + \varepsilon g(x,\varepsilon)$. The behaviour of the transseries depends on both the real and imaginary part of this quantity, in the same fashion as figure 3. The exponential contribution is not present in the transseries in parameter regime ①. In regimes ② and ③ the contribution is present, and must be eight-periodic, due to the value of $\mathrm{Im}[f(\varepsilon)]$ in these regimes. In regime ②, the eight-periodic contribution is small, due to the positive sign of $\mathrm{Re}[f(\varepsilon)]$, and this contribution becomes significant in regime ③, as the sign of $\mathrm{Re}[f(\varepsilon)]$ becomes negative.

does not contribute to the solution, as discussed for the four-periodic case in section 2.2.2. This eight-periodic contribution appears in the transseries as $\varepsilon$ moves into region ②. In this range of $\varepsilon$, there are eight-periodic contributions to the solution, but they are smaller than the four-periodic solution contribution, as the exponential term is relatively small compared to those in $S(x,\varepsilon)$, decaying exponentially as $x \to \infty$. Finally, in region ③, the eight-periodic solution grows exponentially, and the behaviour of $T(x,\varepsilon)$ dominates the solution behaviour.

It is therefore clear that we can explain the onset of these higher periodicity solutions by explicitly studying the exponential weights of the transseries solution; while the algebraic complexity of the process increases after each doubling, the steps for identifying this behaviour remain essentially the same. The resummed transseries therefore provides a systematic approach to studying bifurcations even for larger values of the bifurcation parameter, where classical asymptotic methods typically fail.

## 3. Dynamical logistic equation

In the previous section, we studied the classical logistic equation, and showed that the higher periodicity solutions may be obtained directly using a transseries approach. In this section, we consider a more complicated variant of this problem, known as the slowly-varying logistic equation.

$$y(n+1) = (\lambda_0 + \varepsilon n)y(n)[1 - y(n)], \quad 0 < y(0) < 1, \tag{63}$$

with $\varepsilon > 0$. The bifurcation parameter is given by $\lambda = \lambda_0 + \varepsilon n$, and in this case, it changes slowly over time. In previous studies [30, 32, 34], this has been shown as an example of a 'canard' solution, in which the behaviour appears to remain near the unstable solution for an extended period of time, before rapidly jumping to approach the stable solution with higher periodicity. As $n$ increases, this parameter will pass through values across which the solution stability is known to change. When $\lambda_0 + \varepsilon n = 3$, the one-periodic equilibrium becomes unstable, and the two-periodic equilibrium becomes stable. As $n$ increases further, eventually $\lambda$ exceeds $1 + \sqrt{6}$, and the two-periodic equilibrium becomes unstable, with the four-periodic equilibrium becoming stable. This process continues until the bifurcation parameter becomes sufficiently large that the solution becomes chaotic. For the problem studied here, we will set $\lambda_0 = 3$ and $y(0) = 2/3$.

In [42], it was shown that a discrete multiple scales approach can be used to describe this behaviour asymptotically. This approach required balancing several different timescales, and using asymptotic matching to connect the solutions in each different asymptotic region.

In this section, we will show that this process can be described using a transseries approach, with the resulting expansion to be valid even as the solution behaviour changes dramatically, and increases in periodicity. We will now show that transseries provide a systematic and generally more accurate approach than the multiple scales procedure of [42] in describing the solution behaviour as it transitions from an unstable to a stable manifold; this will demonstrate that transseries expansions can be used to effectively capture canard behaviour in discrete systems.

We will show the first stability transition in detail. We will subsequently provide an outline of how this method can be extended to describe the second transition, together with some results; however, the algebraic manipulations for this process are quite involved, and the precise details will be omitted.

### *3.1. Two-periodic solution*

*3.1.1. Transseries ansatz.* The difference from (9) above is that in the prefactor of the rhs the perturbative parameter $\varepsilon$ is replaced now by $x$. We again begin by applying a multiple scales ansatz, and expanding as a transseries in a continuous variable $x$. Setting $x = \varepsilon n$ and $R(x) = y(n)$ gives

$$R(x + \varepsilon) = (3 + x)R(x)[1 - R(x)], \qquad R(0) = 2/3. \tag{64}$$

We again formulate an ansatz for the solution in terms of $\varepsilon$ and a transseries parameter $\sigma_0$. The ansatz is identical to that given in (10), but has been included below for convenience:

$$R(x, \varepsilon; \sigma_0) = \sum_{m=0}^{\infty} \sigma_0^m \, \mathrm{e}^{-mA(x)/\varepsilon} R_m(x, \varepsilon), \qquad R_m(x, \varepsilon) \simeq \varepsilon^{\beta_m} \sum_{k=0}^{\infty} \varepsilon^k R_{m,k}(x), \tag{65}$$

where $\beta_m$ will again be chosen such that $R_{m,0}$ takes nonzero value. It is straightforward to compute the first few terms of the algebraic portion of the series expression, corresponding to $m = 0$ in (65), which gives a power series expression for the aperiodic manifold. The recursion relation is given obtained by expanding $R(x + \varepsilon)$ using a power series in $\varepsilon$, and matching powers of $\varepsilon$ in the resultant expression. This process gives

$$R_{0,0}(x) = \frac{2 + x}{3 + x}, \tag{66}$$

$$R_{0,k}(x) = -\frac{1}{(2+x)}\left[\sum_{n=1}^{k}\frac{1}{n!}R^{(n)}_{0,k-n}(x) + (3+x)\sum_{n=1}^{k-1}R_{0,n}(x)R_{0,k-n}(x)\right], \quad k \geqslant 1. \tag{67}$$

The first few iterations of this recurrence relation give

$$\begin{aligned} R_{0,1}(x) &= -\frac{1}{(x+2)(x+3)^2}, \qquad R_{0,2}(x) = \frac{x^2+x-4}{(x+2)^3(x+3)^3}, \\ R_{0,3}(x) &= -\frac{x^4-2x^3-28x^2-33x+24}{(x+2)^5(x+3)^4}. \end{aligned} \tag{68}$$

This process may be continued indefinitely in order to continue calculating terms in the power series for the aperiodic manifold. This process will not, however, capture the transition to the two-periodic manifold. In order to obtain an approximation for this behaviour, we are required to consider terms in the ansatz (65) with $m \neq 0$. Continuing to the next order in $\sigma_0\,\mathrm{e}^{-A(x)/\varepsilon}$, we find that

$$\mathrm{e}^{-[A(x+\varepsilon)-A(x)]/\varepsilon}R_1(x+\varepsilon,\varepsilon) = (3+x)R_1(x,\varepsilon)[1-2R_0(x,\varepsilon)]. \tag{69}$$

As before, the argument of the exponential may be determined by expanding $R_1$ as a power series in $\varepsilon$, as well as expanding $A(x+\varepsilon) = A(x) + \varepsilon A'(x) + \cdots$. At leading order in $\varepsilon$, this gives the differential equation

$$\mathrm{e}^{-A'(x)} = -(x+1) = \mathrm{e}^{-(2p+1)\pi\mathrm{i}+\log(x+1)}, \quad p \in \mathbb{Z}. \tag{70}$$

Hence, we obtain

$$A(x) = (2p+1)\pi\mathrm{i}x + x - (x+1)\log(x+1), \tag{71}$$

where we follow the same reasoning as the analysis used to determine (14), and absorb the constant into the series parameter. We may again set $p = 0$; this choice will have no effect on the behaviour of the solution for integer values of $n$.

Once $A(x)$ has been determined, it is possible to obtain a recurrence relation for $R_m(x)$ by applying the first ansatz expression in (65) to the governing equation (64), and matching powers of the transseries parameter $\sigma_0$. This gives

$$\begin{aligned} &(-1)^m(1+x+\varepsilon)^m\,\mathrm{e}^{m((1+x)\log(1+\varepsilon/(1+x))/\varepsilon-1)}R_m(x+\varepsilon,\varepsilon) \\ &\qquad = (3+x)R_m(x,\varepsilon)[1-2R_0(x,\varepsilon)] - (3+x)\sum_{n=1}^{m-1}R_n(x,\varepsilon)R_{m-n}(x,\varepsilon). \end{aligned} \tag{72}$$

It is now possible to apply the second part of the ansatz in (65) and to match powers of $\varepsilon$ in this expression. By direct substitution, we find that $\beta_m = m$ gives the result that $R_{m,0}$ is nonzero. By subsequently matching terms which are $\mathcal{O}(\varepsilon)$ in the small $\varepsilon$ limit, it is possible to generate an equation for $R_{1,0}$ and a recurrence relation for $R_{m,0}$ for $m \geqslant 2$. We find that

$$(x+1)R'_{1,0}(x) = -\left(\frac{2}{x+2} - \frac{2}{x+3} + \frac{1}{2}\right)R_{1,0}, \tag{73}$$

The initial condition in (73) may be chosen arbitrarily, as this choice may be absorbed into the transseries parameter. Choosing $R_{1,0}(0) = 1$ gives

$$R_{1,0}(x) = \frac{3(x+2)^2}{4(x+1)^{3/2}(x+3)}. \tag{74}$$

The recurrence relation for subsequent terms is given by

$$\left[(-1)^m(1+x)^m + (1+x)\right] R_{m,0}(x) = -(3+x)\sum_{n=1}^{m-1} R_{n,0}(x)R_{m-n,0}(x), \quad m \geqslant 2. \tag{75}$$

Continuing to match higher powers of $\varepsilon$ allows for the direct computation of terms further terms such as $R_{m,k}$, obtained by matching terms which are $\mathcal{O}(\varepsilon^k)$ in the small $\varepsilon$ limit. The direct computation of further terms is not required for the present analysis.

*3.1.2. Computing terms in the resummed transseries.* Motivated by the analysis of the static system, and in particular the form of (19), we switch the order of summation in the transseries (65), writing it as

$$R(x,\varepsilon;\sigma_0) \simeq \sum_{k=0}^{\infty} \varepsilon^k \sum_{m=0}^{\infty} \left(\sigma_0 \varepsilon\, \mathrm{e}^{-A(x)/\varepsilon}\right)^m R_{m,k}. \tag{76}$$

A significant difference between this and the static system is that the expansion in powers of $\varepsilon$ here is asymptotic, while the sum over the exponentials ($m \geqslant 0$) is convergent. Thus (76) is a formal expansion.

As for the static system, we define a new series parameter $\tau_0$, and new quantities $\Omega_k(\tau_0)$ such that

$$\tau_0 = \sigma_0 \varepsilon\, \mathrm{e}^{-A(x)/\varepsilon}, \qquad \Omega_k(\tau_0) = \sum_{m=0}^{\infty} \tau_0^m R_{m,k}. \tag{77}$$

It will be helpful later to note that

$$\tau_0(x+\varepsilon) = \mathrm{e}^{-(A(x+\varepsilon)-A(x))/\varepsilon}\tau_0(x) = \tau_0(x)\left[\mathrm{e}^{-A'(x)} + \mathcal{O}(\varepsilon)\right] \quad \text{as } \varepsilon \to 0. \tag{78}$$

The transseries expression in (76) is now given by

$$R(\tau_0,\varepsilon) \simeq \sum_{k=0}^{\infty} \varepsilon^k \Omega_k(\tau_0). \tag{79}$$

We can now apply this expression to (64) and match orders of $\varepsilon$. At leading order, we find that

$$\Omega_0\left(\mathrm{e}^{-A'(x)}\tau_0\right) = (3+x)\Omega_0(\tau_0)(1-\Omega_0(\tau_0)), \tag{80}$$

where (78) was used to obtain the leading-order on the left-hand side. At this stage, we could mechanically obtain the function $\Omega_0$ as a Taylor series in $\tau_0$, which is convergent, with some finite radius of convergence. It happens, however, that there exists a particularly convenient variable transformation that converts the right-hand side from a dilation to a translation. If we define a new variable $y$ such that $y = -x\log(\tau_0)/A'(x)$, the expression in (80) becomes

$$\Omega_0(y+x) = (3+x)\Omega_0(y)(1-\Omega_0(y)). \tag{81}$$

This expression has the same form as the static logistic map equation, given in (9), with $x$ in place of $\varepsilon$. Furthermore, since $x = \varepsilon n$, it is valid to apply the asymptotic solution derived for this expression in section 2.1. As we are interested in capturing the first transition, across which the solution switches from having no periodic component to having a two-periodic component, we can directly apply the transseries expression for the two-periodic solution given in (21).

In order to take into account the form of (81), we must replace $\varepsilon$ and $x$ with $x$ and $y$ respectively in (21). We must also replace the $\tau_0$ in this expression with a new transseries parameter $\overline{\tau}_0$, in which $\varepsilon$ and $x$ are again replaced with $x$ and $y$ respectively. This gives

$$\overline{\tau}_0(y,x) = \overline{\sigma}_0\sqrt{x}\,\mathrm{e}^{-\mathrm{i}\pi y/x + y\,\log(1+x)/x} = \overline{\sigma}_0\sqrt{x}\mathrm{e}^{(\mathrm{i}\pi+\log(1+x))\log(\tau_0)/A'(x)} = \overline{\sigma}_0\sqrt{x}\tau_0, \tag{82}$$

where $\overline{\sigma}_0$ is a new transseries parameter that remains to be determined. Making the appropriate substitutions in (21) now gives the form of $\Omega_0(y)$ as

$$\Omega_0(y) = \frac{2+x}{3+x} + \sqrt{x}\sum_{k=0}^{\infty} x^k\Omega_{\mathrm{o},k}(\overline{\tau}_0) + x\sum_{k=0}^{\infty} x^k\Omega_{\mathrm{e},k}(\overline{\tau}_0), \tag{83}$$

where $\Omega_{\mathrm{o},k}$ and $\Omega_{\mathrm{e},k}$ are defined in (20), and $\Omega_{\mathrm{o},k}$ and $\Omega_{\mathrm{e},k}$ for $k = 0$ and $k = 1$ are given explicitly in (23) and (25) respectively.

In a typical problem of this form, $\overline{\sigma}_0$ would be determined using the fact that $\Omega_0 = 2/3$ at $y = 0$; however, this is enforced by the transformation $y = -x\log(\tau_0)/A'(x)$, which forces $x$ to be zero if $y = 0$. Consequently, the initial condition cannot be used to determine $\overline{\sigma}_0$. This is to be expected, as the initial condition will instead be used to determine the original transseries parameter $\sigma_0$.

Instead, we expand (83) as a Taylor series about $x = 0$ using the form of $\Omega_{\mathrm{o},0}$ and $\Omega_{\mathrm{e},0}$ given in (23). This gives

$$\Omega_0(y) = \frac{2+x}{3+x} + \overline{\sigma}_0 x\tau_0 - \frac{3}{2}(\overline{\sigma}_0 x\tau_0)^2 + \cdots, \tag{84}$$

where the omitted terms are $\mathcal{O}(x^3\tau_0^2)$. We may now match powers of $\tau_0$ with (76) to determine that $x\overline{\sigma}_0 = R_{1,0}$, which was explicitly calculated in (74). We therefore find that

$$\overline{\sigma}_0 = \frac{3(x+2)^2}{4x(x+1)^{3/2}(x+3)}. \tag{85}$$

*3.1.3. Initial condition.* We have now explicitly calculated all of the required quantities for the transseries approximation except for $\sigma_0$, which must be determined from the initial condition at $x = 0$. At $x = 0$, it follows that $\tau_0 = \sigma_0\varepsilon$. Consequently, the initial condition is given by $R(\tau_0 = \sigma_0\varepsilon, x = 0) = 2/3$, which we apply to the first expression in (65). We then express $\sigma_0$ as a power series in $\varepsilon$, where the series terms are functions of $R_{m,k}$ for various values of $m$ and $k$, giving

$$\sum_{m=0}^{\infty}\sigma_0^m R_m(0,\varepsilon), \quad \text{where} \quad \sigma_0 = \sum_{j=0}^{\infty}\varepsilon^j\sigma_{0,j}. \tag{86}$$

Using the second expression from (65) and matching powers of $\varepsilon$ allows us to compute $\sigma_{0,j}$. We have obtained enough $R_{m,k}$ terms to solve for $\sigma_{0,0}$, giving

$$\sigma_0 = -R_{0,1} + \mathcal{O}(\varepsilon) = \frac{1}{18} + \mathcal{O}(\varepsilon). \tag{87}$$

Computing subsequent series terms for $\sigma_0$ requires values of $R_{m,k}$ that are not presented in this study, as even this first order approximation is sufficiently accurate as we now show.

### 3.2. Four-periodic solution

From figure 1, we see that as $n$ increases, eventually the bifurcation parameter becomes sufficiently large that the solution becomes four-periodic. As discussed in section 2.2.2, this higher periodicity must be encoded in the transseries solution as the weights of new exponential scales. We will not perform a full explicit calculation here, but we will demonstrate that these exponential weights do, in fact, predict the emergence of stable behaviour with higher periodicity.

We include a new term with transseries parameter $\sigma_1$, and the analysis suggests that it is natural to define a new scaled variable $z = 2n\varepsilon$. This new contribution to the transseries, denoted $S(z, \varepsilon; \sigma_1)$, is given by

$$S(z, \varepsilon; \sigma_1) = \sum_{m=0}^{\infty} \sigma_1^m \, \mathrm{e}^{-mB(z)/\varepsilon} S_m(z, \varepsilon). \tag{88}$$

By adding $S$ as a perturbation to the two-period solution approximated by (91) and balancing terms in (64) in a similar fashion to section 3.1.1, we obtain an equation for $B(z)$ that gives

$$\begin{aligned} B(z) = -\pi \mathrm{i} z + z - \frac{z}{2} \log(1 - z(4 + z)) \\ + (\sqrt{5} - 2) \log\left(\frac{\sqrt{5} - 2}{\sqrt{5} - 2 - z}\right) - (\sqrt{5} + 2) \log\left(\frac{\sqrt{5} + 2}{\sqrt{5} + 2 + z}\right), \end{aligned} \tag{89}$$

where the constant of integration is picked to set $B(0) = 0$ for convenience, though this choice may be absorbed into the parameter $\sigma_1$. The behaviour of $B(z)$ is depicted in figure 7. There are two significant conclusions that may be drawn from this figure. In figure 7(b), we see that

$$\mathrm{Im}[B'(z)] = \begin{cases} -\pi & z < \sqrt{5} - 2 \\ -3\pi/2 & z > \sqrt{5} - 2 \end{cases} \tag{90}$$

Noting the format of (88), we see that this exponent changes from two-periodic behaviour to four-periodic behaviour when crossing the value $z = \sqrt{5} - 2$. This change in exponent gives rise to four different branches in the solution, and therefore explains the onset of four-periodic behaviour in the solution to the dynamical logistic equation.

The second important observation is that this four-periodicity is not immediately apparent in the solution, due to the behaviour of $\mathrm{Re}[z]$. In figure 7(a), we see that there is a value of $z$, denoted $z_0$ and located at $z_0 \approx 0.9951$, at which the real part of $B(z)$ changes sign from positive to negative. From the form of (88), we see that this corresponds to the four-periodic transseries contribution being exponentially small for $z < z_0$, before growing to have a significant impact on the solution behaviour for $z > z_0$.

This value of $z_0$ corresponds to four-periodic behaviour becoming apparent at $n \approx 0.4975/\varepsilon$. For example, in figure 1, we would expect that four-periodic solution to become significant at $n \approx 3455$, which is consistent with the appearance of the second transition region in this image.

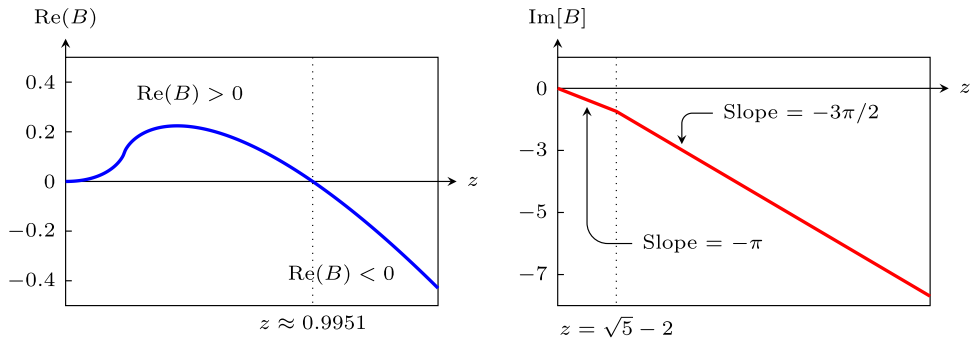


(a) Real part of $B(z)$ (b) Imaginary part of $B(z)$

**Figure 7.** This figure shows the real and imaginary parts of $B(z)$, corresponding to the exponential weight from (89). The periodicity of this contribution may be determined by identifying the slope of the imaginary part, corresponding to $\mathrm{Im}[B'(z)]$. For $z < \sqrt{5} - 2$, the weight $B(z)$ contains an imaginary term $-\pi\mathrm{i}$, which corresponds to two-periodic behaviour. After $z$ exceeds $\sqrt{5} - 2$, the slope of the imaginary term changes to $-3\pi\mathrm{i}/2$, which leads to the appearance of four-periodic behaviour. This behaviour is not immediately apparent, as the contribution is exponentially small if $\mathrm{Re}[z] > 0$, corresponding to $z < z_0$, where $z_0 \approx 0.9951$. For $z > z_0$, the four-periodic terms become significant in the solution behaviour. We note that, due to the bifurcation delay, this behaviour is not immediately visibly apparent in the solution; however, a careful analysis of the corresponding transseries terms will identify the transition between two-periodic and four-periodic behaviour.

A more detailed transseries analysis would permit us to calculate a series approximation for the four-periodic behaviour; however, as we expected from the transseries approach, a straightforward analysis of the exponential weights in the transseries is sufficient to explain the onset of the higher periodicity, and identify the location in $z$ (and hence, in $n$) where this transition to dominant four-periodic behaviour takes place.

Finally, we note that the points where the periodicity changes correspond to values of $n$ where the real part of the exponential weights changes sign, or $z_0$ in figure 7. In asymptotic analysis, this corresponds to the crossing of a curve known as an anti-Stokes curve. This suggests that the Stokes phenomenon plays a role in this system behaviour, in a similar fashion to the continuous delayed bifurcations in [38]. In fact, the solution does contain Stokes curves that are responsible for appearance of exponential factors in the solution; however, finding these Stokes curves requires continuing the solution in the negative-$n$ direction, and was therefore not presented here. Nonetheless, the study the Stokes phenomenon in the dynamic logistic map is an interesting and rich subject which is beyond the scope of the present work.

### *3.3. Error comparison*

From the preceding analysis, we may derive an approximation for the solution to the slowly-varying logistic equation (64), which we denote $R_{\mathrm{app}}$. This approximation may be validated against numerical simulations, as well as the multiple scales method developed in [42].

Combining (20), (77), (82), (83), (85) and (87), we find an approximation for the transseries solution that describes the onset of two-periodic behaviour in the solution. This approximation

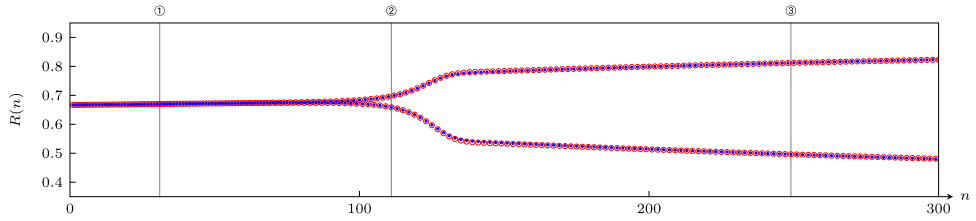


(a) Exact solution (red circles) and transseries approximation (blue dots) for $\varepsilon = 0.001$.

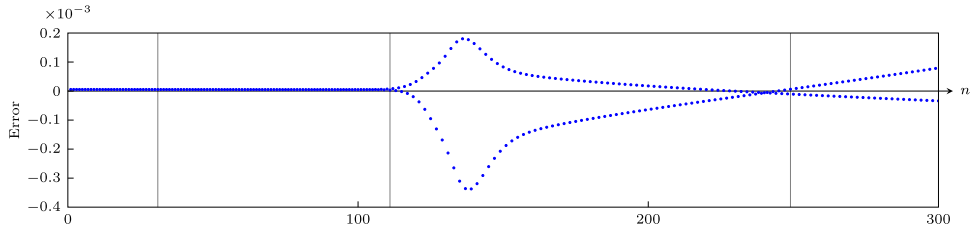


(b) Approximation error for $\varepsilon = 0.001$.

**Figure 8.** The plot in (a) shows the approximation (91) and exact solution of (63) for $\varepsilon = 0.001$. The difference between these is shown in (b). The points labeled ①, ②, and ③ will be referenced below in figure 9. We see that the error reaches a maximum at the start of the two-periodic regime. It then decreases, although will eventually increase as $n$ grows, due to the increasing influence of the four-periodic region which was not computed. Note that the error is equal to zero near the point labelled ③. This corresponds to the value where the approximation crosses the exact solution, which occurs at some point in the two-periodic region for any choice of $\varepsilon$ and therefore does not signify a special parameter choice. It is an artifact of the error calculation.

is given by

$$R(x) \approx R_{\text{app}}(x) = \frac{2+x}{3+x} + x^{1/2}\Omega_{\text{o},0}(\overline{\tau}_0) + x\Omega_{\text{e},0}(\overline{\tau}) + x^{3/2}\Omega_{\text{o},1}(\overline{\tau}_0) + x^2\Omega_{\text{e},1}(\overline{\tau}_0), \tag{91}$$

where

$$\overline{\tau}_0 \approx \frac{\epsilon(x+2)^2\,\mathrm{e}^{-(\pi \mathrm{i}x + x - (x+1)\log(x+1))/\varepsilon}}{24x^{1/2}(x+1)^{3/2}(x+3)}. \tag{92}$$

The most useful feature of this approximation is that it is valid before, during, and after the transition region from aperiodic to two-periodic behaviour in the slowly-varying logistic equation. We illustrate an example comparison in figure 8(a), corresponding to $\varepsilon = 0.001$. The approximation is shown as blue dots, and overlaid on top of the exact solution, shown as red circles. The two solutions are visually almost indistinguishable.

The approximation error for this example is shown in figure 8(b), calculated by $y(n) - R_{\text{app}}(\varepsilon n)$. The error reaches a peak following the transition region, at the beginning of the stable two-periodic behaviour. The error does grow in this region as $n$ becomes large, and continues to do so until the transition to four-periodic behaviour occurs. This behaviour is not depicted in figure 8(b).

In order to obtain a more complete picture of the accuracy of the transseries approximation, we determined the approximation error at three selected values of $n$. These values were tested in [42] relative to other methods, to obtain representative computations of the approximation error

in important parts of the solution domain. The first point is $n = \lfloor 1/\sqrt{\varepsilon} \rfloor$. This point is found in the early aperiodic region before the transition from aperiodic behaviour to two-periodic behaviour occurs. It is labelled ① in the example solution from figure 8.

For comparison, we need to identify the remaining representative points used in [42], which required the computation of an intermediate quantity $K$, satisfying

$$K = \sqrt{\log K - \frac{3}{2}\log(\varepsilon)}. \tag{93}$$

This quantity was derived in [42] although it has been adjusted to take into account the slightly different form for the slowly-varying logistic equation considered here. The second point falls within the transition region between the aperiodic unstable manifold and the two-periodic stable manifold, and is given by $n = \lfloor K + K^{-1}/\sqrt{\varepsilon} \rfloor$. This point is labelled ② in the example solution from figure 8. Finally, we also determine the error at a point in the region where the solution has completed its transition to two-periodic stable behaviour. This point is given by $n = \lfloor K + 15K^{-1}/\sqrt{\varepsilon} \rfloor$, and is labelled ③ in the example solution from figure 8. The error for each of these three points was studied in [42] allowing for direct comparison between the transseries approximation and the multiple scales approximation errors.

The error for each of the three representative points over a range of $\varepsilon$ values may be seen in figure 9, shown in blue. The error for the approximation from the multiple scales approximation in [42] is shown in red for each point. In each region, both approximations are relatively accurate. In the aperiodic region, the multiple scales approximation outperforms the transseries approximation, while in the transition and two-periodic region, the transseries approximation is substantially more accurate.

This outcome is sensible; the transseries approximation tracks the contribution of exponentials in the solution, and accurately incorporates them into the solution behaviour. In the aperiodic region, the solution is best represented by an algebraic power series in $\varepsilon$. The multiple scales approach involves calculating this power series to several terms, while our transseries approximation relies only on the leading-order behaviour of this series. In the transition and two-periodic region, however, these exponential contributions become more significant, and this corresponds to the transseries approximation becoming more accurate than the multiple scales approximation. While the multiple scales approximation is able to capture some of the exponential behaviour, the transseries approximation is able to incorporate several exponential corrections in a straightforward fashion, producing greater accuracy in the solution regions where these corrections play an important role. Furthermore, increasing the accuracy of the transseries approximation in the aperiodic region can be done systematically by including higher corrections in $\varepsilon$.

Finally, we note that there are points in figures 9(b) and (c) where the error appears to drop to zero. This corresponds to a coincidental crossing between the approximation and actual solution occurring at this value of $n$. The crossing may be seen in the example solution from 8 at $n \approx 250$. Any solution with a reasonable amount of accuracy will have some value of $n$ where this crossing occurs; this does not provide any added insight into the accuracy of the approximation.

## 4. Discussion

We have obtained transasymptotic approximations for the solutions to both the standard and slowly varying logistic equation. In each case, we were able not only to reproduce the results calculated in [42] using multiple scales asymptotic methods, but to go significantly further.

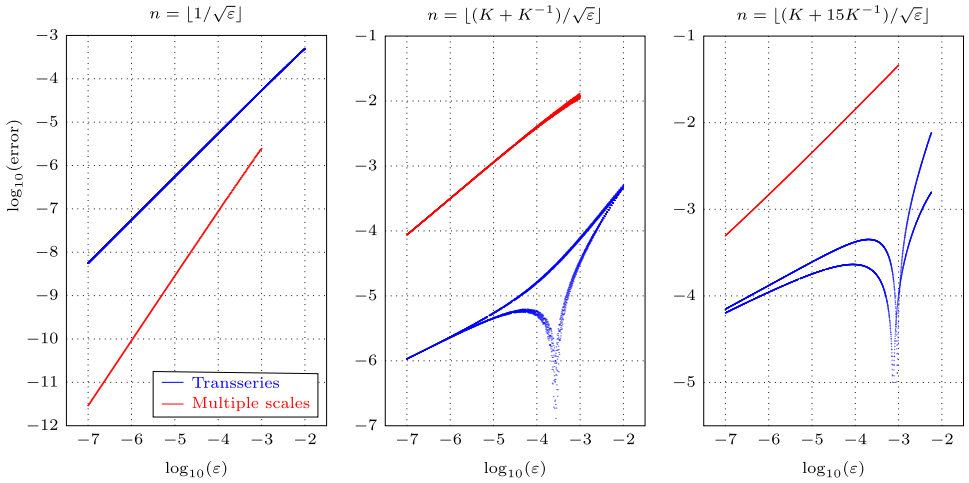


(a) Aperiodic region at ① (b) Transitional region at ② (c) Two-periodic region at ③

**Figure 9.** This figure shows the error in the dynamic system at the three points identified in [42] as belonging to the inner region, transition region, and outer region, shown as points ①, ②, and ③ in figure 8. In each case, the error is shown as a blue curve. This curve becomes smaller as $\varepsilon$ decreases. The point at which the error dips is an artifact of the observation that the approximation crosses the exact solution at the identified point for this choice of $\varepsilon$, and does not represent any significant phenomenon within the transseries approximation. The cause of this behaviour is explained in more detail within the description of figure 8. We have chosen a similar range of small parameter to the analysis in [42], shown in red. The transseries outperforms the multiple scales method in both the transition region and the outer region, in which the exponential terms play an important role in describing the solution behaviour. These terms are more naturally captured using transseries methods, leading to an improved approximation.

As, *a priori*, transseries methods allow for the straightforward calculation of higher-order exponentials, the transseries approximation was able to represent the solution more accurately than the multiple scales method both during and after the delayed bifurcation, as seen in figure 9; during and after the bifurcation, the initially subdominant exponentials contribute significantly to the solution, so it should be expected that the transseries approximation would be particularly accurate compared to other methods in these regions.

Furthermore, the transseries approach can still provide a useful approximation when the parameter $\varepsilon$ is not particularly small, as the solution can simply be rescaled to determine the next asymptotic weight.

We considered the dynamic logistic equation with $\varepsilon > 0$, producing a cascade of delayed bifurcations. If $\varepsilon < 0$, causing the bifurcation parameter to decrease rather than increase, bifurcations appear earlier than the solution stability would suggest, rather than later [8]. A transseries approach could be used in almost identical fashion to the present study in order to approximate these accelerated bifurcations; however, that analysis is beyond the scope of this study.

There are several significant and general advantages to the transseries resummation approach. The first is that the method we have described can be applied in systematic fashion to a wide range of problems, including both discrete and continuous systems. Whilst such advantages have already been seen elsewhere, in the context of the logistic equation it has been

instructive to compare this to the multiple scales approach from [42], which required the careful comparison of asymptotic terms up to several orders. In order to capture the fast discrete scale, as well as both the inner and outer continuous scales near the bifurcation, asymptotic matching was performed through three scales.

The transseries approach here was able to reproduce this behaviour by resumming the series in order to ensure that the transasymptotic approximation contained behaviour encoded in the subdominant exponentials; this behaviour contained all of the information found using asymptotic matching methods. Furthermore, improving approximation accuracy by computing more terms of a multiple scales expansion requires comparing the asymptotic behaviour of more terms and checking to determine when the relative dominance of terms changes, while obtaining a more accurate transseries expression simply requires the systematic calculation of further series terms in the transseries. While these calculations can prove challenging, the steps required to obtain the subdominant exponentials, and the associated solution behaviour, follow the same consistent process at each stage which it is applied.

Computing the subdominant exponentials is not valuable simply in that it produces a more accurate approximation. In fact, a second major advantage of the transseries method is that the exponential weights have a significant effect on the system behaviour, and computing just these weights can tell us the form of the solution as parameters in the problem vary. In our analysis of the standard logistic map, we showed that two-, four-, and eight-periodic behaviour can be determined simply by carefully studying the subdominant weights. This explains the appearance of higher periodicities in the solution, and suggests that if this process is continued, it can be used to study further bifurcations in the period doubling process.

In our subsequent analysis of the period doubling cascade found in the slowly varying logistic equation, we were able to predict the onset of two-periodic and four-periodic behaviour in the solution, simply by studying the relative size of the exponential weights associated with the two- and four-periodic contributions. It would be particularly interesting to continue to investigate how the full period doubling cascade is encoded in the exponential weights of this system, and whether this can provide (at least theoretically) further insight into the period doubling route to chaos.

Transseries methods have been used to study Stokes phenomenon in a wide range of continuous problems. Given that multiple scales methods have been used to study Stokes phenomenon in discrete problems [1, 46–50], it is likely that the transseries approach described here could be used to provide new insight into discrete variants of Stokes phenomenon.

Finally the full analysis of the movements of exponential contributions between Riemann sheets, seen in the dynamic logistic map, also merits further investigation. Examples of such phenomena have been observed recently in novel features of aeroacoustic flows [60, 61]. Initial explorations appear to suggest this is commonly found in other physical and mathematical contexts.

## Acknowledgments

IA has been supported by the UK EPSRC Early Career Fellowship EP/S004076/1, and the FCT-Portugal Grant PTDC/MAT-OUT/28784/2017. CJL has been supported by Australian Research Council Discovery Project #190101190. DH has been supported by the presidential scholarship of the University of Southampton. The authors thank Dr Cameron Hall for helpful discussions.

## Appendix A. Explicit transseries terms

In (21), the transseries for $R(\tau_0, \varepsilon)$ is written in terms of a base approximation $R_0(\varepsilon)$, a sum of odd terms in $\tau_0$, denoted $\Omega_{\mathrm{o},k}$, and a sum of even terms in $\tau_0$, denoted $\Omega_{\mathrm{e},k}$. We further simplify this by writing $R(\tau_0, \varepsilon; \sigma_0) = R(\varepsilon) + S(\tau_0, \varepsilon)$, where

$$S(\tau_0, \varepsilon) = \sqrt{\varepsilon} \sum_{k=0}^{\infty} \varepsilon^k \Omega_{\mathrm{o},k}(\tau_0) + \varepsilon \sum_{k=0}^{\infty} \varepsilon^k \Omega_{\mathrm{e},k}(\tau_0). \tag{94}$$

We note that $\tau_0(x + \varepsilon) = -(1 + \varepsilon)\tau_0(x)$. Consequently,

$$S(\tau_0(x + \varepsilon), \varepsilon) = S(-(1 + \varepsilon)\tau_0(x), \varepsilon). \tag{95}$$

Applying (94) and (95) to the logistic equation (9) gives

$$S(-(1 + \varepsilon)\tau_0, \varepsilon) = -(1 + \varepsilon)S(\tau_0, \varepsilon) - (3 + \varepsilon)S(\tau_0, \varepsilon)^2. \tag{96}$$

Expanding the left-hand side of this expression as a Taylor series in $\varepsilon$ gives

$$\begin{aligned} S(-(1 + \varepsilon)\tau_0, \varepsilon) &= \sum_{j=0}^{\infty} \frac{(-\tau_0 \varepsilon)^j}{j!} R^{(j)}(-\tau_0) \\ &= -\sqrt{\varepsilon} \sum_{m=0}^{\infty} \varepsilon^m \sum_{k=0}^{m} \frac{\tau_0^k}{k!} \Omega^{(k)}_{\mathrm{o},m-k}(\tau_0) + \varepsilon \sum_{m=1}^{\infty} \varepsilon^n \sum_{k=0}^{m-1} \frac{\tau_0^k}{k!} \Omega^{(k)}_{\mathrm{e},n-1-k}(\tau_0), \end{aligned} \tag{97}$$

where we used the fact that $\Omega_{\mathrm{o},k}$ and $\Omega_{\mathrm{e},k}$ are odd and even in $\tau_0$ respectively. The remaining expansions in (96) may be obtained by substitution of (94) into (96). It is straightforward to show that

$$R(\tau_0, \varepsilon)^2 = 3 \sum_{m=1}^{\infty} \varepsilon^m \sum_{k=0}^{m-1} \Omega_{\mathrm{o},k}(\tau_0) \Omega_{\mathrm{o},m-1-k}(\tau_0) \tag{98}$$

$$+\sqrt{\varepsilon} \sum_{m=1}^{\infty} \varepsilon^m \sum_{k=0}^{m-1} \Omega_{\mathrm{o},k}(\tau_0) \Omega_{\mathrm{e},m-1-k}(\tau_0) + \sum_{m=2}^{\infty} \varepsilon^m \sum_{k=0}^{m-2} \Omega_{\mathrm{e},k}(\tau_0) \Omega_{\mathrm{e},m-2-k}(\tau_0). \tag{99}$$

These expansions may now be used to equate powers of $\varepsilon$ and obtain the expressions given in (23) and (25).

## Appendix B. Initial condition for four-periodic equation

In order to calculate the initial condition for the four-periodic problem, we first recall that $\hat{R}(x, \varepsilon)$ was derived in order to satisfy the initial condition for small $\epsilon$. The four-periodic solution arises for $\varepsilon > -2 + \sqrt{6}$, or $\eta > 0$. Hence, we determine the initial condition by perturbing around the leading-order behaviour of $\hat{R}(x, \varepsilon)$, which is initially two-periodic for the parameter regime under consideration. We then determine $\sigma_1$ by matching with the initial condition in the limit that $\eta \to 0$.

We first obtain stable two-periodic behaviour of $R(x, \varepsilon)$ from (8), letting $x = 0$ in order to describe the initial state. This expression may be written in terms of $\eta$, to allow a small $\eta$ expansion in this limit. This gives

$$\hat{R}(0,\varepsilon) = \frac{4+\varepsilon+\sqrt{\varepsilon(4+\varepsilon)}}{2(3+\varepsilon)} \sim \frac{1}{5}\left(2-\sqrt{3}+\sqrt{2+\sqrt{3}}\right) + \frac{\eta}{50}\left(3\sqrt{2}-16\sqrt{3}-7\sqrt{6}+12\right) + \frac{3\eta^2}{250}\left(-47\sqrt{2}+84\sqrt{3}+18\sqrt{6}-38\right)+\mathcal{O}(\eta^3). \tag{100}$$

Setting $x = 0$, letting $\sigma_1 = \sigma_{1,0} + \eta\sigma_{1,1} + \cdots$, and expanding $S$ in powers of $\eta$ gives

$$S(0,\varepsilon) \sim \eta\sigma_{1,0} + \eta^2\left(-\frac{5}{12}(14-7\sqrt{2}-4\sqrt{3}+4\sqrt{6})\sigma_{1,0}^3 + (3\sqrt{3}-\sqrt{6}+\frac{3}{2}\sqrt{2}-1)\sigma_{1,1}^2+\sigma_1\right)+\mathcal{O}(\eta^3). \tag{101}$$

To determine the appropriate initial condition, we fix the case for $\eta = 0$, which gives

$$R(0,\varepsilon) = \frac{1}{5}\left(2-\sqrt{3}+\sqrt{2+\sqrt{3}}\right). \tag{102}$$

By setting $R(0,\varepsilon) = \hat{R}(0,\varepsilon) + S(0,\varepsilon)$, and matching powers of $\eta$, we can obtain

$$\sigma_1 = -\frac{1}{50}\left(3\sqrt{2}-16\sqrt{3}-7\sqrt{6}+12\right) + \frac{\eta}{500}\left(297\sqrt{2}-709\sqrt{3}-189\sqrt{6}+399\right)+\mathcal{O}(\eta^2), \tag{103}$$

This is sufficient information to approximate the solution using the transseries behaviour, although it is straightforward to continue this process to obtain higher corrections for $\sigma_1$.

## ORCID iDs

Inês Aniceto https://orcid.org/0000-0002-4468-0066
Daniel Hasenbichler https://orcid.org/0000-0002-5390-5175
Christopher J Howls https://orcid.org/0000-0001-7989-7807
Christopher J Lustri https://orcid.org/0000-0001-9504-277X

## References

[1] Alfimov G L, Korobeinikov A S, Lustri C J and Pelinovsky D E 2019 Standing lattice solitons in the discrete NLS equation with saturation *Nonlinearity* **32** 3445
[2] Aniceto I, Başar G and Schiappa R 2019 A primer on resurgent transseries and their asymptotics *Phys. Rep.* **809** 1–135
[3] Aniceto I, Jankowski J, Meiring B and Spaliński M 2019 The large proper-time expansion of Yang–Mills plasma as a resurgent transseries *J. High Energy Phys.* JHEP02(2019)073
[4] Aniceto I and Schiappa R 2015 Nonperturbative ambiguities and the reality of resurgent transseries *Commun. Math. Phys.* **335** 183–245
[5] Aniceto I, Schiappa R and Vonk M 2012 The resurgence of instantons in string theory *Commun. Number Theory Phys.* **6** 339
[6] Aniceto I, Schiappa R and Vonk M 2021 Quadratic transasymptotics for Painlevé zeroes: from 2D quantum gravity to the matrix model (to appear) (http://online.kitp.ucsb.edu/online/resurgent_c17/vonk )

[7] Baesens C 1991 Noise effect on dynamic bifurcations: the case of a period-doubling cascade *Dynamic Bifurcations* (Berlin: Springer) pp 107–30

[8] Baesens C 1991 Slow sweep through a period-doubling cascade: delayed bifurcations and renormalisation *Physica* D **53** 319–75

[9] Basar G and Dunne G V 2015 Resurgence and the Nekrasov–Shatashvili limit: connecting weak and strong coupling in the Mathieu and Lamé systems *J. High Energy Phys.* JHEP02(2015)160

[10] Benoît É, Fruchard A, Schäfke R and Wallet G 1998 Solutions surstables des équations différentielles complexes lentes-rapides à point tournant *Ann. Fac. Sci. Toulouse, Math.* **7** 627–58

[11] Berry M V 1989 Uniform asymptotic smoothing of Stokes's discontinuities *Proc. R. Soc.* A **422** 7–21

[12] Casalderrey-Solana J, Gushterov N I and Meiring B 2018 Resurgence and hydrodynamic attractors in Gauss–Bonnet holography *J. High Energy Phys.* JHEP04(2018)042

[13] Costin O 1995 Exponential asymptotics, transseries, and generalized Borel summation for analytic, nonlinear, rank-one systems of ordinary differential equations *Int. Math. Res. Not.* **1995** 377–417

[14] Costin O 1998 On Borel summation and Stokes phenomena for rank-1 nonlinear systems of ordinary differential equations *Duke Math. J.* **93** 289–344

[15] Costin O and Costin R D 2001 On the formation of singularities of solutions of nonlinear differential systems in antistokes directions *Invent Math.* **145** 425–85

[16] Costin O, Costin R D and Huang M 2015 Tronquée solutions of the Painlevé equation PI *Constr. Approx.* **41** 467–94

[17] Costin O and Dunne G V 2019 Resurgent extrapolation: rebuilding a function from asymptotic data. Painlevé I *J. Phys. A: Math. Theor.* **52** 445205

[18] Costin O and Dunne G V 2020 Uniformization and constructive analytic continuation of Taylor series (arXiv:2009.01962 )

[19] Couso-Santamaría R, Edelstein J D, Schiappa R and Vonk M 2015 Resurgent transseries and the holomorphic anomaly: nonperturbative closed strings in local $\mathbb{CP}^2$ *Commun. Math. Phys.* **338** 285–346

[20] Couso-Santamaria R, Schiappa R and Vaz R 2015 Finite $N$ from resurgent large $N$ *Ann. Phys., NY* **356** 1–28

[21] Davies H G and Rangavajhula K 1997 Dynamic period-doubling bifurcations of a unimodal map *Proc. R. Soc.* A **453** 2043–61

[22] Davies H G and Rangavajhula K 2001 A period-doubling bifurcation with slow parametric variation and additive noise *Proc. R. Soc.* A **457** 2965–82

[23] Davies H G and Rangavajhula K 2002 Noisy parametric sweep through a period-doubling bifurcation of the Hénon map *Chaos Solitons Fractals* **14** 293–9

[24] Demulder S, Dorigoni D and Thompson D C 2016 Resurgence in $\eta$-deformed principal chiral models *J. High Energy Phys.* JHEP07(2016)088

[25] d'Escurac P P 2017 The Borel transform of canard values and its singularities *FASdiff: Formal and Analytic Solutions of Diff. (Differential, Partial Differential, Difference, q-Difference, q-Difference-Differential,…) Equations* (Berlin: Springer) pp 149–75

[26] Dorigoni D and Kleinschmidt A 2020 Resurgent expansion of Lambert series and iterated Eisenstein integrals *Commun. Num. Theor. Phys.* **15** 1–57

[27] Dunne G V and Ünsal M 2014 Uniform WKB, multi-instantons, and resurgent trans-series *Phys. Rev.* D **89** 105009

[28] Eckhaus W 1983 Relaxation oscillations including a standard chase on French ducks *Asymptotic Analysis II* (*Lecture Notes in Mathematics* )vol 985) (Berlin: Springer) pp 449–97

[29] Edgar G A 2009 Transseries for beginners *Real Anal. Exch.* **35** 253–310

[30] El-rabih A 2003 Canards solutions of difference equations with small step size *J. Differ. Equ. Appl.* **9** 911–31

[31] Fruchard A 1991 Existence of bifurcation delay: the discrete case *Dynamic Bifurcations* (Berlin: Springer) pp 87–106

[32] Fruchard A 1996 Sur l'équation aux différences affine du premier ordre unidimensionnelle *Ann. Inst. Fourier* **46** 139–81

[33] Fruchard A and Schäfke R 2003 Bifurcation delay and difference equations *Nonlinearity* **16** 2199

[34] Fruchard A and Schäfke R 2009 A survey of some results on overstability and bifurcation delay *Discrete Continuous Dyn. Syst.* S **2** 931

[35] Garoufalidis S, Gu J and Mariño M 2020 The resurgent structure of quantum knot invariants (arXiv:2007.10190 )

[36] Garoufalidis S, Its A, Kapaev A and Mariño M 2012 Asymptotics of the instantons of Painlevé I *Int. Math. Res. Not.* **2012** 561–606
[37] Gelfreich V and Sauzin D 2001 Borel summation and splitting of separatrices for the Hénon map *Ann. Inst. Fourier* **51** 513–67
[38] Goh R, Kaper T J and Vo T 2020 Delayed Hopf bifurcation and space-time buffer curves in the complex Ginzburg–Landau equation (arXiv:2012.10048 )
[39] Grassi A and Gu J 2019 Argyres–Douglas theories, Painlevé II and quantum mechanics *J. High Energy Phys.* JHEP02(2019)060
[40] Grassi A, Mariño M and Zakany S 2015 Resumming the string perturbation series *J. High Energy Phys.* JHEP05(2015)038
[41] Hakim V and Mallick K 1993 Exponentially small splitting of separatrices, matching in the complex plane and borel summation *Nonlinearity* **6** 57–70
[42] Hall C L and Lustri C J 2016 Multiple scales and matched asymptotic expansions for the discrete logistic equation *Nonlinear Dyn.* **85** 1345–62
[43] Heller M P and Spaliński M 2015 Hydrodynamics beyond the gradient expansion: resurgence and resummation *Phys. Rev. Lett.* **115** 072501
[44] Howls C J 2010 Exponential asymptotics and boundary-value problems: keeping both sides happy at all orders *Proc. R. Soc.* A **466** 2771–94
[45] Howls C J, Langman P J and Olde Daalhuis A B 2004 On the higher-order Stokes phenomenon *Proc. R. Soc.* A **460** 2285–303
[46] Joshi N and Lustri C J 2015 Stokes phenomena in discrete Painlevé I *Proc. R. Soc.* A **471** 20140874
[47] Joshi N and Lustri C J 2019 Generalized solitary waves in a finite-difference Korteweg–de Vries equation *Stud. Appl. Math.* **142** 359–84
[48] Joshi N, Lustri C J and Luu S 2017 Stokes phenomena in discrete Painlevé II *Proc. R. Soc.* A **473** 20160539
[49] Joshi N, Lustri C J and Luu S 2019 Nonlinear q-Stokes phenomena for q-Painlevé I *J. Phys. A: Math. Theor.* **52** 065204
[50] King J R and Chapman S J 2001 Asymptotics beyond all orders and Stokes lines in nonlinear differential-difference equations *Eur. J. Appl. Math.* **12** 433
[51] Mariño M and Reis T 2020 Resurgence and renormalons in the one-dimensional Hubbard model (arXiv:2006.05131 )
[52] Mariño M, Schiappa R and Weiss M 2009 Multi-instantons and multicuts *J. Math. Phys.* **50** 052301
[53] Martín P, Sauzin D and Seara T M 2011 Exponentially small splitting of separatrices in the perturbed McMillan map *Discrete Continuous Dyn. Syst.* A **31** 301
[54] Olde Daalhuis A B 2004 Inverse factorial-series solutions of difference equations *Proc. Edinburgh Math. Soc.* **47** 421–48
[55] Olde Daalhuis A B 2005 Hyperasymptotics for nonlinear ODEs: I. A Riccati equation *Proc. R. Soc.* A **461** 2503–20
[56] Olde Daalhuis A B 2005 Hyperasymptotics for nonlinear ODEs: II. The first Painlevé equation and a second-order Riccati equation *Proc. R. Soc.* A **461** 3005–21
[57] Pasquetti S and Schiappa R 2010 Borel and Stokes nonperturbative phenomena in topological string theory and $c = 1$ matrix models *Ann. Henri Poincaré* **11** 351
[58] Schiappa R and Vaz R 2014 The resurgence of instantons: multi-cut Stokes phases and the Painlevé II equation *Commun. Math. Phys.* **330** 655–721
[59] Shudo A and Ikeda K S 2008 Stokes geometry for the quantum Hénon map *Nonlinearity* **21** 1831–80
[60] Stone J T, Self R H and Howls C J 2017 Aeroacoustic catastrophes: upstream cusp beaming in Lilley's equation *Proc. R. Soc.* A **473** 20160880
[61] Stone J T, Self R H and Howls C J 2018 Cones of silence, complex rays and catastrophes: high-frequency flow-acoustic interaction effects *J. Fluid Mech.* **853** 37–71
[62] Tabor M 1989 *Chaos and Integrability in Nonlinear Dynamics: An Introduction* (New York: Wiley)
[63] Wechselberger M 2012 À propos de canards (Apropos canards) *Trans. Am. Math. Soc.* **364** 3289–309